A FULLY DIVERGENCE-FREE FINITE ELEMENT METHOD FOR MAGNETOHYDRODYNAMIC EQUATIONS

RALF HIPTMAIR

Seminar of Applied Mathematics, Swiss Federal Institute of Technology
Zurich, CH-8092, Switzerland
ralfh@ethz.ch

LINGXIAO LI

NCMIS, LSEC, Institute of Computational Mathematics and Scientific/Enginnering Computing, Academy of Mathematics and Systems Science, Chinese Academy of Sciences
School of Mathematical Science, University of Chinese Academy of Sciences
Beijing, 100190, China
lilingxiao@lsec.cc.ac.cn

SHIPENG MAO

NCMIS, LSEC, Institute of Computational Mathematics and Scientific/Enginnering Computing, Academy of Mathematics and Systems Science, Chinese Academy of Sciences
School of Mathematical Science, University of Chinese Academy of Sciences
Beijing, 100190, China
maosp@lsec.cc.ac.cn

WEIYING ZHENG

NCMIS, LSEC, Institute of Computational Mathematics and Scientific/Enginnering Computing, Academy of Mathematics and Systems Science, Chinese Academy of Sciences
School of Mathematical Science, University of Chinese Academy of Sciences
Beijing, 100190, China
zwy@lsec.cc.ac.cn

We propose a finite element method for the three-dimensional transient incompressible magnetohydrodynamic equations that ensures exactly divergence-free approximations of the velocity and the magnetic induction. We employ second-order semi-implicit timestepping, for which we rigorously establish an energy law and, as a consequence, unconditional stability. We prove unique solvability of the linear systems of equations to be solved in every timestep. For those we design an efficient preconditioner so that the number of preconditioned GMRES iterations is uniformly bounded with respect to the number of degrees of freedom As both meshwidth and timestep size tend to zero, we prove that the discrete solutions converge to a weak solution of the continuous problem. Finally, by several numerical experiments, we confirm the predictions of the theory and demonstrate the efficiency of the preconditioner.

Keywords: Magnetohydrodynamic equations; divergence-free finite element method; preconditioner; magnetic vector potential; driven cavity flow.

AMS Subject Classification: 65M60, 76W05

1. Introduction

The incompressible magnetohydrodynamic (MHD) equations describe the dynamic behavior of an electrically conducting fluid under the influence of a magnetic field. They occur in models for, fusion reactor blankets, liquid metal magnetic pumps, aluminum electrolysis among others (see Refs. [1,26]). MHD is a multi-physics phenomenon: the magnetic field changes the momentum of the fluid through the Lorenz force, and conversely, the conducting fluid influences the magnetic field through electric currents. In this way multiple physical fields, such as the velocity, the pressure, and the electromagnetic fields, are coupled.

In this paper, we study the incompressible MHD equations in a bounded domain $\Omega \subset \mathbb{R}^3$ with connected boundary. They comprise the incompressible Navier-Stokes equations and the magnetoquasistatic Maxwell's equations

$$\frac{\partial \boldsymbol{u}}{\partial t} + (\boldsymbol{u} \cdot \nabla)\boldsymbol{u} + \nabla p - \nu \Delta \boldsymbol{u} - \boldsymbol{J} \times \boldsymbol{B} = \boldsymbol{f} \qquad \text{in } \Omega, \tag{1.1a}$$

$$\frac{\partial \boldsymbol{B}}{\partial t} + \mathbf{curl}\, \boldsymbol{E} = 0 \qquad \text{in } \Omega, \tag{1.1b}$$

$$\mathbf{curl}\, \boldsymbol{H} = \boldsymbol{J} \qquad \text{in } \Omega, \tag{1.1c}$$

$$\operatorname{div} \boldsymbol{u} = 0, \qquad \operatorname{div} \boldsymbol{B} = 0 \qquad \text{in } \Omega, \tag{1.1d}$$

where $\boldsymbol{u}$ is the fluid velocity, p is the hydrodynamic pressure, $\boldsymbol{E}$ is the electric field, $\boldsymbol{H}$ is the magnetic field, $\boldsymbol{B}$ is the magnetic induction, $\boldsymbol{J}$ is the electric current density, and $\boldsymbol{f} \in \boldsymbol{L}^2(\Omega)$ stands for external force. The equations in (1.1) are complemented with the following constitutive equation and Ohm's law

$$\boldsymbol{B} = \mu \boldsymbol{H}, \qquad \boldsymbol{J} = \sigma(\boldsymbol{E} + \boldsymbol{u} \times \boldsymbol{B}). \tag{1.2}$$

The physical parameters are, respectively, the kinematic viscosity ν, the magnetic permeability μ, and the electric conductivity σ. For the well-posedness of (1.1) and (1.2), we assume the following initial and boundary conditions

$$\begin{aligned} &\boldsymbol{u}(0) = \boldsymbol{u}_0, \quad && \boldsymbol{B}(0) = \boldsymbol{B}_0 \qquad && \text{in } \Omega, \\ &\boldsymbol{u} = 0, && \boldsymbol{E} \times \boldsymbol{n} = 0 && \text{on } \Gamma := \partial\Omega. \end{aligned} \tag{1.3}$$

Numerical methods for incompressible MHD equations have been studied widely. For the stationary model, we refer to Refs. [10, 15, 16, 31] for stabilized and mixed finite element methods. In Ref. [16], the authors proved optimal error estimates for $\boldsymbol{H}^1(\Omega)$-conforming finite element approximations both to velocity $\boldsymbol{u}$ and magnetic induction $\boldsymbol{B}$ in either convex polyhedra or domains with $C^{1,1}$-smooth boundaries. It is well-known that $\boldsymbol{B}$ may not be in $\boldsymbol{H}^1(\Omega)$ in general Lipschitz domains which are not convex. In Ref. [31], Schötzau proved the well-posedness of stationary MHD equations and studied a mixed finite element method which discretizes $\boldsymbol{u}$

with $\boldsymbol{H}^1(\Omega)$-conforming finite elements and $\boldsymbol{B}$ with $\boldsymbol{H}(\mathbf{curl},\Omega)$-conforming finite elements. The mixed finite element method yields a discrete magnetic induction $\boldsymbol{B}_h$ which is weakly divergence free, that is, $\boldsymbol{B}_h$ is orthogonal to all discrete gradient fields. In Ref. [14], Greif, Li, Schötzau, and Wei extended the framework by focusing on the conservation of mass, namely, $\operatorname{div}\boldsymbol{u} = 0$. They proposed a mixed discontinuous Galerkin (DG) finite element method for the stationary MHD model and discretized $\boldsymbol{u}$ in an $\boldsymbol{H}(\operatorname{div},\Omega)$-conforming finite element space. The merit of the method is that the discrete velocity satisfies $\operatorname{div}\boldsymbol{u}_h = 0$ exactly. In Ref. [30] A. Prohl proved the convergence of discrete solutions for time-dependent MHD equations where $\boldsymbol{B}$ is descretized with $\boldsymbol{H}(\mathbf{curl},\Omega)$-conforming edge elements.

In recent years, exactly divergence-free approximations for $\boldsymbol{B}$ have attracted more and more interest in the context of spatial discretization of the time-dependent MHD equations. We would like to mention a simulation code for fusion reactor blankets (cf. Refs. [1,2]) and the current density-conservative finite volume methods of Ni et al. for the inductionless MHD model on both structured and unstructured grids (cf. Refs. [28,29,35,38]). These methods are efficient for high Hartmann numbers and have been validated by experimental results. In Ref. [21], in contrast to most existing approaches that eliminate the electrical field variable $\boldsymbol{E}$ and give a direct discretization of the magnetic field, the authors discretize the electric field $\boldsymbol{E}$ by Nédélec's edge elements and discretize the magnetic induction $\boldsymbol{B}$ by Raviart-Thomas face elements. In this way, $\operatorname{div}\boldsymbol{B}_h = 0$ is ensured exactly for the discrete solution. In Ref. [22], they also propose a robust preconditioner for solving the discrete problem.

The main objective of this paper is to propose a new *mixed DG finite element method* for solving (1.1). Inspired by Ref. [14], we approximate the velocity $\boldsymbol{u}$ by $\boldsymbol{H}(\operatorname{div},\Omega)$-conforming finite elements and the pressure p by fully discontinuous finite elements. As a result, the conservation of mass is satisfied exactly on the discrete level, that is, $\operatorname{div}\boldsymbol{u}_h = 0$ holds in strong sense. The divergence-free property of $\boldsymbol{B}$ is realized by means of a magnetic vector potential. Instead of solving for $\boldsymbol{B}$, we solve for the magnetic vector potential $\boldsymbol{A}$ such that

$$\mathbf{curl}\,\boldsymbol{A} = \boldsymbol{B}, \qquad \boldsymbol{E} = -\frac{\partial \boldsymbol{A}}{\partial t}.$$

Approximating the magnetic vector potential by $\boldsymbol{H}(\mathbf{curl},\Omega)$-conforming edge elements and defining $\boldsymbol{B}_h = \mathbf{curl}\,\boldsymbol{A}_h$, we find that $\operatorname{div}\boldsymbol{B}_h = 0$ holds naturally. Thus our mixed finite element method is *fully divergence-free* in the sense that both the discrete velocity and the discrete magnetic induction satisfy exactly

$$\operatorname{div}\boldsymbol{u}_h = 0, \qquad \operatorname{div}\boldsymbol{B}_h = 0.$$

To establish the convergence of discrete solutions, we follow Ref. [30] and show the existence subsequences of discrete solutions which converge weakly to the exact solutions $(\boldsymbol{u},\boldsymbol{A})$ as the meshwidth h and timestep τ tend to zero. These convergence results do not hinge on any assumptions about the regularity of solutions. Moreover, as a by-product we obtain is the existence of weak solutions of the MHD evolution problem. The proof of convergence rates for the discrete solutions requires to assume higher regularity of the true solutions and is fairly technical (cf. [18,30,36] for finite element approximations of the $\boldsymbol{B}$-based MHD formulation). It is not covered in this manuscript.

The second objective of the paper is to propose an efficient solver for the systems of equations faced in every timestep. In the spirit of semi-implicit timestepping we pursue a linearization at t_n by extrapolating the discrete solutions from t_{n-1} and t_{n-2}. Thus we need only solve linear systems of equations at each time step. Existence and uniqueness of their solutions can be shown and a *discrete energy law* holds for the fully discrete scheme. Numerical experiments reveal that the extrapolated scheme is second order in time. Both properties imply that the proposed method is stable and efficient for long-time simulation of MHD problems.

We also propose a preconditioner for solving the linear systems of equations in each timestep. The optimality of the preconditioner is verified numerically with respect to the number of degrees of freedom (DOFs). Extensive numerical experiments are presented to verify the convergence rate of the mixed finite element method and the optimality of the preconditioner, to demonstrate the competitive performance of the linear extrapolated scheme, and to validate the $\boldsymbol{A}$-based MHD formulation for an engineering benchmark problem. Furthermore, our numerical results well match the two-dimensional simulations for a driven cavity flow in Ref. [23].

The paper is organized as follows: In Section 2, we introduce the MHD model which relies on the velocity, the pressure, and the vector magnetic potential as unknowns. A weak formulation is proposed and an energy law of for its solutions is established. In Section 3, we propose a fully discrete mixed DG finite element method for solving the weak MHD formulation using the extrapolation of the solutions from previous time steps. The energy law for the discrete solutions is shown. In Section 4, we prove that, in the sense of extracted subsequences, the discrete solutions converge to $(\boldsymbol{u}, \boldsymbol{A})$ which satisfy the continuous MHD equations in weak sense. Consequently, we have actually proven the existence of weak solutions. In Section 5, we introduce a preconditioned GMRES algorithm for solving the discrete problems. In Section 6, we present five numerical experiments to test the predictions of the theory and to demonstrate the competitive performance of the MHD solver.

2. A weak formulation of the MHD model

The purpose of this section is to derive a weak formulation of the MHD system (1.1) based on the vector magnetic potential. An energy law for the solutions is also proven. Throughout the paper, we assume that $\Omega \subset \mathbb{R}^3$ is a bounded, simply-connected, and Lipschitz polyhedral domain with boundary $\Gamma = \partial\Omega$. For simplicity, we assume that the density of fluid $\rho \equiv 1$ and the physical parameters μ, σ, ν are positive constants. Moreover, vector-valued quantities will be denoted by boldface notations, such as $\boldsymbol{L}^2(\Omega) := (L^2(\Omega))^3$.

Let $L^2(\Omega)$ be the space of square-integrable functions and let its inner product and norm be denoted by

$$(u, v) := \int_\Omega uv, \qquad \|u\|_{L^2(\Omega)} := (u, u)^{1/2}.$$

We shall also use the usual Hilbert spaces like $H^1(\Omega)$, $\boldsymbol{H}(\mathbf{curl}, \Omega)$, $\boldsymbol{H}(\mathrm{div}, \Omega)$ and their subspaces $H_0^1(\Omega)$, $\boldsymbol{H}_0(\mathbf{curl}, \Omega)$, $\boldsymbol{H}_0(\mathrm{div}, \Omega)$ with vanishing traces, vanishing tangential traces, and vanishing normal traces on Γ respectively. We refer to Chapter 3 in Ref. [25] for their definitions and inner products. The subspaces of curl-free functions and divergence-free functions are denoted by

$$\begin{aligned}
\boldsymbol{H}(\mathrm{div}\,0, \Omega) &:= \{\boldsymbol{v} \in \boldsymbol{H}(\mathrm{div}, \Omega) \,:\, \mathrm{div}\,\boldsymbol{v} = 0\}, \\
\boldsymbol{H}_0(\mathrm{div}\,0, \Omega) &:= \{\boldsymbol{v} \in \boldsymbol{H}_0(\mathrm{div}, \Omega) \,:\, \mathrm{div}\,\boldsymbol{v} = 0\}.
\end{aligned}$$

Since $\mathrm{div}\,\boldsymbol{B} = 0$, we can introduce a magnetic vector potential $\boldsymbol{A}$ and write

$$\boldsymbol{E} = -\frac{\partial \boldsymbol{A}}{\partial t}, \quad \boldsymbol{B} = \mathbf{curl}\,\boldsymbol{A} \qquad \text{in } \Omega, \tag{2.1}$$

where the *temporal gauge* is adopted for convenience. With the abbreviations $\partial_t \boldsymbol{u} = \dfrac{\partial \boldsymbol{u}}{\partial t}$ and $\partial_t \boldsymbol{A} = \dfrac{\partial \boldsymbol{A}}{\partial t}$, (1.1) can be written as follows

$$\begin{aligned}
\partial_t \boldsymbol{u} + (\boldsymbol{u} \cdot \nabla)\boldsymbol{u} + \nabla p - \nu \Delta \boldsymbol{u} - \boldsymbol{J} \times \mathbf{curl}\,\boldsymbol{A} &= \boldsymbol{f} && \text{in } \Omega, \\
\mathrm{div}\,\boldsymbol{u} &= 0 && \text{in } \Omega, \\
\sigma\left(\partial_t \boldsymbol{A} + \mathbf{curl}\,\boldsymbol{A} \times \boldsymbol{u}\right) + \mathbf{curl}\,\mu^{-1}\,\mathbf{curl}\,\boldsymbol{A} &= 0 && \text{in } \Omega, \\
-\sigma\left(\partial_t \boldsymbol{A} + \mathbf{curl}\,\boldsymbol{A} \times \boldsymbol{u}\right) &= \boldsymbol{J} && \text{in } \Omega.
\end{aligned}$$

Using (1.3) and (2.1), it suffices to set the initial condition for $\boldsymbol{A}$ by solving the static problem

$$\mathbf{curl}\,\boldsymbol{A}_0 = \boldsymbol{B}_0, \quad \mathrm{div}\,\boldsymbol{A}_0 = 0 \qquad \text{in } \Omega, \tag{2.3}$$

$$\boldsymbol{A}_0 \times \boldsymbol{n} = 0 \qquad \text{on } \Gamma. \tag{2.4}$$

The boundary condition for $\boldsymbol{A}$ can be obtained by combining (1.3) and (2.1)

$$\boldsymbol{A} \times \boldsymbol{n} = \boldsymbol{A}_0 \times \boldsymbol{n} - \int_0^t (\boldsymbol{E} \times \boldsymbol{n}) = 0 \qquad \text{on } \Gamma.$$

For simplicity, let U_0, B_0, L_0 be the characteristic quantities for velocity, magnetic induction, and the length of the system respectively. We introduce the following scalings

$$\begin{aligned}
&\boldsymbol{x} \leftarrow \boldsymbol{x}/L_0, \quad && t \leftarrow tU_0/L_0, \quad && \boldsymbol{A} \leftarrow \boldsymbol{A}/(B_0 L_0), \\
&\boldsymbol{u} \leftarrow \boldsymbol{u}/U_0, \quad && p \leftarrow p/U_0^2, \quad && \boldsymbol{f} \leftarrow \boldsymbol{f} L_0/U_0^2.
\end{aligned}$$

Then, the MHD system can be written in a dimensionless form

$$
\begin{aligned}
\partial_t \boldsymbol{u} + \boldsymbol{u}\cdot\nabla\boldsymbol{u} + \nabla p - R_e^{-1}\Delta\boldsymbol{u} - \kappa\boldsymbol{J}\times\mathbf{curl}\,\boldsymbol{A} &= \boldsymbol{f} \quad \text{in } \Omega, && \text{(2.5a)}\\
\operatorname{div}\boldsymbol{u} &= 0 \quad \text{in } \Omega, && \text{(2.5b)}\\
\partial_t \boldsymbol{A} + \mathbf{curl}\,\boldsymbol{A}\times\boldsymbol{u} + R_m^{-1}\,\mathbf{curl}\,\mathbf{curl}\,\boldsymbol{A} &= 0 \quad \text{in } \Omega, && \text{(2.5c)}\\
-\partial_t \boldsymbol{A} - \mathbf{curl}\,\boldsymbol{A}\times\boldsymbol{u} &= \boldsymbol{J} \quad \text{in } \Omega, && \text{(2.5d)}\\
\boldsymbol{u}(0) = \boldsymbol{u}_0, \quad \boldsymbol{A}(0) &= \boldsymbol{A}_0 \quad \text{in } \Omega, && \text{(2.5e)}\\
\boldsymbol{u} = 0, \quad \boldsymbol{A}\times\boldsymbol{n} &= 0 \quad \text{on } \Gamma, && \text{(2.5f)}
\end{aligned}
$$

Now we derive a weak formulation of (2.5). For the sake of brevity, we introduce some notations for function spaces

$$
\begin{aligned}
\boldsymbol{V} &:= \boldsymbol{H}_0^1(\Omega), & \boldsymbol{V}(\operatorname{div}0) &:= \boldsymbol{V}\cap\boldsymbol{H}(\operatorname{div}0,\Omega),\\
\boldsymbol{C} &:= \boldsymbol{H}_0(\mathbf{curl},\Omega), & \boldsymbol{C}(\operatorname{div}0) &:= \boldsymbol{C}\cap\boldsymbol{H}(\operatorname{div}0,\Omega).
\end{aligned}
$$

Multiply both sides of (2.5a) with $\boldsymbol{v}\in\boldsymbol{V}(\operatorname{div}0)$. Using integration by parts and noting that $\boldsymbol{v}=0$ on Γ, we have

$$
(\partial_t\boldsymbol{u} + \boldsymbol{u}\cdot\nabla\boldsymbol{u} - \kappa\boldsymbol{J}\times\mathbf{curl}\,\boldsymbol{A}, \boldsymbol{v}) + R_e^{-1}(\nabla\boldsymbol{u},\nabla\boldsymbol{v}) = (\boldsymbol{f},\boldsymbol{v}).
$$

Substituting (2.5d) into the above equality, we get

$$
(\partial_t\boldsymbol{u} + \boldsymbol{u}\cdot\nabla\boldsymbol{u}, \boldsymbol{v}) + \kappa(\partial_t\boldsymbol{A} + \mathbf{curl}\,\boldsymbol{A}\times\boldsymbol{u}, \mathbf{curl}\,\boldsymbol{A}\times\boldsymbol{v}) + \frac{1}{R_e}(\nabla\boldsymbol{u},\nabla\boldsymbol{v}) = (\boldsymbol{f},\boldsymbol{v}).
$$

Multiplying both sides of (2.5c) with $\boldsymbol{\varphi}\in\boldsymbol{C}$ and integrating by part, we have

$$
(\partial_t\boldsymbol{A} + \mathbf{curl}\,\boldsymbol{A}\times\boldsymbol{u}, \boldsymbol{\varphi}) + \frac{1}{R_m}(\mathbf{curl}\,\boldsymbol{A}, \mathbf{curl}\,\boldsymbol{\varphi}) = 0.
$$

With the abbreviations

$$
\mathcal{O}(\boldsymbol{w};\boldsymbol{u},\boldsymbol{v}) := ((\boldsymbol{w}\cdot\nabla)\boldsymbol{u},\boldsymbol{v}), \quad \mathcal{A}(\boldsymbol{v},\boldsymbol{w}) := R_e^{-1}(\nabla\boldsymbol{v},\nabla\boldsymbol{w}), \quad \boldsymbol{u},\boldsymbol{v},\boldsymbol{w}\in\boldsymbol{V},
$$

the desired weak formulation of (2.5) reads:

Find $\boldsymbol{u}\in\boldsymbol{L}^2(0,T;\boldsymbol{V}(\operatorname{div}0))\cap\boldsymbol{W}^{1,r}(0,T;\boldsymbol{V}(\operatorname{div}0)')$ and $\boldsymbol{A}\in\boldsymbol{W}^{1,r}(0,T;\boldsymbol{C})$ such that $\boldsymbol{u}(0)=\boldsymbol{u}_0$, $\boldsymbol{A}(0)=\boldsymbol{A}_0$, and

$$
\begin{aligned}
&(\partial_t\boldsymbol{u},\boldsymbol{v}) + \mathcal{O}(\boldsymbol{u};\boldsymbol{u},\boldsymbol{v}) + \mathcal{A}(\boldsymbol{u},\boldsymbol{v}) + \kappa(\partial_t\boldsymbol{A} + \mathbf{curl}\,\boldsymbol{A}\times\boldsymbol{u}, \mathbf{curl}\,\boldsymbol{A}\times\boldsymbol{v})\\
&\qquad\qquad = (\boldsymbol{f},\boldsymbol{v}) \qquad \forall\,\boldsymbol{v}\in\boldsymbol{V}(\operatorname{div}0), \qquad \text{(2.6a)}\\
&(\partial_t\boldsymbol{A} + \mathbf{curl}\,\boldsymbol{A}\times\boldsymbol{u}, \boldsymbol{\varphi}) + R_m^{-1}(\mathbf{curl}\,\boldsymbol{A}, \mathbf{curl}\,\boldsymbol{\varphi}) = 0 \qquad \forall\,\boldsymbol{\varphi}\in\boldsymbol{C}, \qquad \text{(2.6b)}
\end{aligned}
$$

where $r>1$ is a constant depending only on Ω. The existence of the solutions to problem (2.6) will be discussed in Section 4.

Theorem 2.1. *Let* $(\boldsymbol{u}, \boldsymbol{A})$ *be the solutions of* (2.6) *and define*

$$\boldsymbol{B} := \mathbf{curl}\, \boldsymbol{A}, \qquad \boldsymbol{J} := -\partial_t \boldsymbol{A} - \boldsymbol{B} \times \boldsymbol{u}.$$

Assume $\boldsymbol{A} \in \boldsymbol{H}^1(0,T;\boldsymbol{L}^2(\Omega))$ *and* $\boldsymbol{B} \times \boldsymbol{u} \in \boldsymbol{L}^2(0,T;\boldsymbol{L}^2(\Omega))$. *The energy law*

$$\mathsf{E}(T) + \int_0^T \mathsf{P}(t)\mathrm{d}t = \mathsf{E}(0) + \int_0^T (\boldsymbol{f}, \boldsymbol{u})\, \mathrm{d}t$$

holds, where

$$\begin{aligned} \mathsf{E}(t) &:= \tfrac{1}{2} \|\boldsymbol{u}(t)\|^2_{\boldsymbol{L}^2(\Omega)} + \tfrac{\kappa}{2R_m} \|\boldsymbol{B}(t)\|^2_{\boldsymbol{L}^2(\Omega)}, \\ \mathsf{P}(t) &:= \tfrac{1}{R_e} \|\nabla \boldsymbol{u}(t)\|^2_{\boldsymbol{L}^2(\Omega)} + \kappa \|\boldsymbol{J}(t)\|^2_{\boldsymbol{L}^2(\Omega)}. \end{aligned}$$

Proof. Since $\partial_t \boldsymbol{A}$, $\boldsymbol{B} \times \boldsymbol{u} \in \boldsymbol{L}^2(0,T;\boldsymbol{L}^2(\Omega))$, we have $\boldsymbol{J} \in \boldsymbol{L}^2(0,T;\boldsymbol{L}^2(\Omega))$. Taking $\boldsymbol{\varphi} = \partial_t \boldsymbol{A}$ in (2.6b), we have

$$\frac{1}{2R_m} \frac{\mathrm{d}}{\mathrm{d}t} \|\boldsymbol{B}\|^2_{\boldsymbol{L}^2(\Omega)} = (\boldsymbol{J}, \partial_t \boldsymbol{A}) = -\|\boldsymbol{J}\|^2_{\boldsymbol{L}^2(\Omega)} - (\boldsymbol{J}, \boldsymbol{B} \times \boldsymbol{u}). \tag{2.7}$$

For any $\boldsymbol{w} \in \boldsymbol{V}(\mathrm{div}\, 0)$, since $\mathrm{div}\, \boldsymbol{w} = 0$, direct calculations show that

$$\int_\Omega (\boldsymbol{w} \cdot \nabla)\boldsymbol{u} \cdot \boldsymbol{v} = -\int_\Omega (\boldsymbol{w} \cdot \nabla)\boldsymbol{v} \cdot \boldsymbol{u} \qquad \forall\, \boldsymbol{v} \in \boldsymbol{H}^1_0(\Omega).$$

This means that $\mathcal{O}(\boldsymbol{w}; \boldsymbol{u}, \boldsymbol{u}) = 0$. Taking $\boldsymbol{v} = \boldsymbol{u}$ in (2.6a) shows that

$$\frac{1}{2} \frac{\mathrm{d}}{\mathrm{d}t} \|\boldsymbol{u}\|^2_{\boldsymbol{L}^2(\Omega)} - \kappa(\boldsymbol{J}, \boldsymbol{B} \times \boldsymbol{u}) + \frac{1}{R_e} \|\nabla \boldsymbol{u}\|^2_{\boldsymbol{L}^2(\Omega)} = (\boldsymbol{f}, \boldsymbol{u}). \tag{2.8}$$

Substituting (2.7) into (2.8) yields

$$\frac{1}{2} \frac{\mathrm{d}}{\mathrm{d}t} \|\boldsymbol{u}\|^2_{\boldsymbol{L}^2(\Omega)} + \frac{\kappa}{2R_m} \frac{\mathrm{d}}{\mathrm{d}t} \|\boldsymbol{B}\|^2_{\boldsymbol{L}^2(\Omega)} + \kappa \|\boldsymbol{J}\|^2_{\boldsymbol{L}^2(\Omega)} + \frac{1}{R_e} \|\nabla \boldsymbol{u}\|^2_{\boldsymbol{L}^2(\Omega)} = (\boldsymbol{f}, \boldsymbol{u}).$$

Integrating both sides over $(0,T)$ yields the lemma. □

Remark 2.1. The energy law describes the variation of the total energy caused by energy conversion and the work of external forces. The total energy E consists of the fluid kinetic energy $\frac{1}{2} \|\boldsymbol{u}\|^2_{\boldsymbol{L}^2(\Omega)}$ and the magnetic field energy $\frac{\kappa}{2R_m} \|\boldsymbol{B}\|^2_{\boldsymbol{L}^2(\Omega)}$. The dissipation of E stems from the friction losses $R_e^{-1} \|\nabla \boldsymbol{u}\|^2_{\boldsymbol{L}^2(\Omega)}$ and the Ohmic losses $\kappa \|\boldsymbol{J}\|^2_{\boldsymbol{L}^2(\Omega)}$. The energy supply from external force is represented by $(\boldsymbol{f}, \boldsymbol{u})$.

3. An interior-penalty finite element method

In this section, we study the fully discrete approximation of the MHD equations. The velocity $\boldsymbol{u}$ will be discretized by $\boldsymbol{H}(\mathrm{div}, \Omega)$-conforming finite elements with interior penalties in a DG-type approach. This is inspired by Ref. [14], which presents an interior-penalty finite element method for the $\boldsymbol{B}$-based formulation of stationary MHD model.

3.1. Finite element spaces

Let $\mathcal{T}_h$ be a shape-regular tetrahedral triangulation of Ω and let $\mathcal{F}_h$ be the set of all element faces of $\mathcal{T}_h$. We introduce the space of discontinuous $\mathcal{T}_h$-piecewise polynomials,

$$D_m(\mathcal{T}_h) := \{v \in L^2(\Omega) : v|_K \in P_m(K), K \in \mathcal{T}_h\},$$

where $P_m(K)$ is the space of polynomials with degrees $\leq m$. The $\boldsymbol{H}_0(\mathrm{div}, \Omega)$- and $\boldsymbol{H}_0(\mathbf{curl}, \Omega)$-conforming piecewise linear finite element spaces are defined as follows, c.f. Refs. [27, 34]:

$$\begin{aligned} \boldsymbol{V}_h &= \{\boldsymbol{v} \in \boldsymbol{H}_0(\mathrm{div}, \Omega) : \boldsymbol{v}|_K \in \boldsymbol{P}_1(K),\ K \in \mathcal{T}_h\}, \\ \boldsymbol{C}_h &= \{\boldsymbol{v} \in \boldsymbol{H}_0(\mathbf{curl}, \Omega) : \boldsymbol{v}|_K \in \boldsymbol{P}_1(K),\ K \in \mathcal{T}_h\}. \end{aligned}$$

For convenience, we denote the divergence-free subspace of $\boldsymbol{V}_h$ as follows

$$\boldsymbol{V}_h(\mathrm{div}\,0) := \boldsymbol{V}_h \cap \boldsymbol{H}(\mathrm{div}\,0, \Omega).$$

We use the customary notations in the field of discontinuous Galerkin (DG) methods: We endow each $F \in \mathcal{F}_h$ with a unit normal $\boldsymbol{n}_F$ which points to the exterior of Ω when $F \subset \Gamma$. For any interior face $F \in \mathcal{F}_h$, let K_+, K_- be two adjacent elements of $\mathcal{T}_h$ such that $F = \partial K_+ \cap K_- \in \mathcal{F}_h$. We always assume that $\boldsymbol{n}_F$ points to the exterior of K_+. Let φ be a scalar-, vector-, or matrix-valued function which is piecewise smooth over $\mathcal{T}_h$. The mean value and jump of φ on F are defined respectively by

$$\{\!\{\varphi\}\!\} := (\varphi_+ + \varphi_-)/2, \quad [\![\varphi]\!] := \varphi_+ - \varphi_- \quad \text{on } F,$$

where $\varphi_\pm$ denote the traces of φ on F from inside of $K_\pm$ respectively. For any face $F = \partial K_+ \cap \Gamma$, the mean value and the jump of φ on F are defined by

$$\{\!\{\varphi\}\!\} = [\![\varphi]\!] = \varphi_+ \quad \text{on } F.$$

We shall use the discrete semi-norm and norms

$$\begin{aligned} &\|\varphi\|_{0,h} := \left(\sum_{F\in\mathcal{F}_h} h_F^{-1}\,\|\varphi\|^2_{L^2(F)}\right)^{\frac{1}{2}}, \qquad |\varphi|_{1,h} := \left(\sum_{K\in\mathcal{T}_h} \|\nabla\varphi\|^2_{\boldsymbol{L}^2(K)}\right)^{\frac{1}{2}}, \\ &\|\varphi\|_{1,h} := \left(|\varphi|^2_{1,h} + \|[\![\varphi]\!]\|^2_{0,h}\right)^{\frac{1}{2}}. \end{aligned}$$

Lemma 3.1 (Poincáre's inequality). *For any $1 \leq p \leq 6$, there exists a constant $C(p) > 0$ independent of the meshwidth such that*

$$\|v\|_{L^p(\Omega)} \leq C(p)\,\|v\|_{1,h} \qquad \forall\, v \in D_k(\mathcal{T}_h)\,. \tag{3.1}$$

Proof. The inequality is proven for two-dimensional case in Lemma 6.2 of Ref. [13]. In fact, a careful inspection of its proof shows that it also applies to three-dimensional case. We do not elaborate on the details. For $p = 2$, we also refer to Refs. [4, 7]. □

The discrete counterparts of the bilinear and trilinear forms are defined by

$$\mathcal{A}_h(\boldsymbol{u},\boldsymbol{v}) = \frac{1}{R_e}\sum_{K\in\mathcal{T}_h}\int_K \nabla\boldsymbol{u}:\nabla\boldsymbol{v} + \frac{\alpha}{R_e}\sum_{F\in\mathcal{F}_h} h_F^{-1}\int_F [\![\boldsymbol{u}]\!]\cdot[\![\boldsymbol{v}]\!]$$
$$-\frac{1}{R_e}\sum_{F\in\mathcal{F}_h}\int_F\left(\left\{\!\!\left\{\frac{\partial\boldsymbol{u}}{\partial\boldsymbol{n}}\right\}\!\!\right\}\cdot[\![\boldsymbol{v}]\!] + \left\{\!\!\left\{\frac{\partial\boldsymbol{v}}{\partial\boldsymbol{n}}\right\}\!\!\right\}\cdot[\![\boldsymbol{u}]\!]\right),$$
$$O_h(\boldsymbol{w};\boldsymbol{u},\boldsymbol{v}) = -\sum_{K\in\mathcal{T}_h}\int_K \boldsymbol{u}\cdot\mathrm{div}(\boldsymbol{w}\otimes\boldsymbol{v}) + \sum_{K\in\mathcal{T}_h}\int_{\partial K}(\boldsymbol{w}\cdot\boldsymbol{n}_K)\left(\boldsymbol{u}^{\downarrow}\cdot\boldsymbol{v}\right),$$

where $\alpha > 0$ is the penalty parameter independent of the mesh, $\boldsymbol{n}_K$ is the unit outer normal of ∂K, h_F is the diameter of F, and $\boldsymbol{u}^{\downarrow}$ denotes the upwind convective flux defined by Refs. [9, 14]

$$\boldsymbol{u}^{\downarrow}(\boldsymbol{x}) = \begin{cases}\lim\limits_{\varepsilon\to 0+}\boldsymbol{u}(\boldsymbol{x}-\varepsilon\boldsymbol{w}(x)), & \boldsymbol{x}\in\partial K\backslash\Gamma,\\ 0, & \boldsymbol{x}\in\partial K\cap\Gamma.\end{cases}$$

The following lemma states that $\mathcal{A}_h(\cdot,\cdot)$ is coercive on $\boldsymbol{D}_m(\mathcal{T}_h)$.

Lemma 3.2. *Suppose α is large enough but independent of h_F and R_e. Then there is a constant $\theta_1 > 0$ independent of h_F and R_e such that*

$$R_e\mathcal{A}_h(\boldsymbol{v}_h,\boldsymbol{v}_h) \ge \theta_1\left\|\boldsymbol{v}_h\right\|_{1,h}^2 \qquad \forall\,\boldsymbol{v}_h\in\boldsymbol{D}_m(\mathcal{T}_h).$$

Proof. The proof is standard. We present it here for completeness. By the norm equivalence on finite dimensional space (cf. Lemma A.6 in Ref. [13]), there exists a constant C_1 independent of h_F such that

$$h_F\left\|\nabla\boldsymbol{v}_h\right\|_{\boldsymbol{L}^2(F)}^2 \le C_1\left\|\nabla\boldsymbol{v}_h\right\|_{\boldsymbol{L}^2(K_F)}^2 \qquad \forall\,F\in\mathcal{F}_h,$$

where $K_F\in\mathcal{T}_h$ satisfies $F\subset\partial K_F$. Therefore

$$R_e\mathcal{A}_h(\boldsymbol{v}_h,\boldsymbol{v}_h) = |\boldsymbol{v}_h|_{1,h}^2 + \alpha\left\|[\![\boldsymbol{v}_h]\!]\right\|_{0,h}^2 - 2\sum_{F\in\mathcal{F}_h}\int_F\left\{\!\!\left\{\frac{\partial\boldsymbol{v}_h}{\partial\boldsymbol{n}}\right\}\!\!\right\}\cdot[\![\boldsymbol{v}_h]\!]$$
$$\ge |\boldsymbol{v}_h|_{1,h}^2 + (\alpha-2C_1^2)\left\|[\![\boldsymbol{v}_h]\!]\right\|_{0,h}^2 - \frac{1}{2C_1}\sum_{F\in\mathcal{F}_h}h_F\left\|\{\!\!\{\nabla\boldsymbol{v}_h\}\!\!\}\right\|_{\boldsymbol{L}^2(F)}^2$$
$$\ge \frac{1}{2}|\boldsymbol{v}_h|_{1,h}^2 + (\alpha-2C_1^2)\left\|[\![\boldsymbol{v}_h]\!]\right\|_{0,h}^2.$$

We complete the proof by setting $\alpha > 2C_1^2$ and $\theta_1 := \min(1/2, \alpha-2C_1^2)$. $\square$

Lemma 3.2 states that $\mathcal{A}_h(\cdot,\cdot)$ provides an equivalent norm on $\boldsymbol{D}_m(\mathcal{T}_h)$:

$$\left\|\boldsymbol{v}_h\right\|_{\mathcal{A}_h} := \sqrt{\mathcal{A}_h(\boldsymbol{v}_h,\boldsymbol{v}_h)}.$$

We shall also use the space of piecewise regular functions

$$\boldsymbol{H}^1(\mathcal{T}_h) := \left\{\boldsymbol{v}\in\boldsymbol{L}^2(\Omega):\ \boldsymbol{v}|_K\in\boldsymbol{H}^1(K),\ \ K\in\mathcal{T}_h\right\}.$$

We cite Ref. [9] for the following lemma on the positivity and continuity of the trilinear form $\mathcal{O}_h$. The proof is omitted here.

Lemma 3.3. *Let $\boldsymbol{w}, \boldsymbol{w}_1 \in \boldsymbol{H}^1(\mathcal{T}_h) \cap \boldsymbol{H}(\mathrm{div}\,0, \Omega)$ and $\boldsymbol{v} \in \boldsymbol{D}_m(\mathcal{T}_h)$. Then*

$$\mathcal{O}_h(\boldsymbol{w}; \boldsymbol{v}, \boldsymbol{v}) = \frac{1}{2} \sum_{F \in \mathcal{F}_h} \int_F |\boldsymbol{w} \cdot \boldsymbol{n}| \, |[\![\boldsymbol{v}]\!]|^2 \ .$$

Furthermore, for any $\boldsymbol{u} \in \boldsymbol{H}_0^1(\Omega) + \boldsymbol{D}_m(\mathcal{T}_h)$, there exists a constant C_0 independent of the meshwidth such that

$$|\mathcal{O}_h(\boldsymbol{w}; \boldsymbol{u}, \boldsymbol{v}) - \mathcal{O}_h(\boldsymbol{w}_1; \boldsymbol{u}, \boldsymbol{v})| \leq C_0 \, \|\boldsymbol{w} - \boldsymbol{w}_1\|_{1,h} \, \|\boldsymbol{u}\|_{1,h} \, \|\boldsymbol{v}\|_{1,h} \ .$$

3.2. *A semi-implicit time-stepping scheme*

Now we study the fully discrete approximation to the MHD problem. Let $\{t_n = n\tau : \ n = 0, 1, \cdots, N\}$, $\tau = T/N$, be an equidistant partition of the time interval $[0, T]$. For a sequence of functions $\{\boldsymbol{v}_n\}$, we define the backward difference operator and mean values by

$$\begin{aligned} \delta_t \boldsymbol{v}_n &:= \frac{1}{\tau}(\boldsymbol{v}_n - \boldsymbol{v}_{n-1}), \qquad \bar{\boldsymbol{v}}_n := \frac{1}{2}(\boldsymbol{v}_n + \boldsymbol{v}_{n-1}), \\ \boldsymbol{f}_n &:= \frac{1}{6}\left[\boldsymbol{f}(t_n) + 4\boldsymbol{f}(t_{n-1/2}) + \boldsymbol{f}(t_{n-1})\right] . \end{aligned} \tag{3.2}$$

Let $\mathbf{u}_0 \in \boldsymbol{V}_h(\mathrm{div}\,0)$, $\mathbf{A}_0 \in \boldsymbol{C}_h$ be quasi-interpolations of the initial conditions $\boldsymbol{u}_0$ and $\boldsymbol{A}_0$ respectively (cf. e.g. Ref. [20]).

The Crank-Nicolson scheme for the fully discrete approximation of (2.6) reads:

Find $(\mathbf{u}_n, \mathbf{A}_n) \in \boldsymbol{V}_h(\mathrm{div}\,0) \times \boldsymbol{C}_h$, $n \geq 1$, such that

$$\begin{aligned} &(\delta_t \mathbf{u}_n, \boldsymbol{v}) + \mathcal{O}_h(\bar{\mathbf{u}}_n; \bar{\mathbf{u}}_n, \boldsymbol{v}) + \mathcal{A}_h(\bar{\mathbf{u}}_n, \boldsymbol{v}) \\ &\qquad + \kappa(\delta_t \mathbf{A}_n + \bar{\mathbf{B}}_n \times \bar{\mathbf{u}}_n, \bar{\mathbf{B}}_n \times \boldsymbol{v}) = (\boldsymbol{f}_n, \boldsymbol{v}) \qquad \forall\, \boldsymbol{v} \in \boldsymbol{V}_h(\mathrm{div}\,0), \end{aligned} \tag{3.3a}$$

$$\big(\delta_t \mathbf{A}_n + \bar{\mathbf{B}}_n \times \bar{\mathbf{u}}_n, \boldsymbol{c}\big) + R_m^{-1}(\mathbf{curl}\,\bar{\mathbf{A}}_n, \mathbf{curl}\,\boldsymbol{c}) = 0 \qquad \forall\, \boldsymbol{c} \in \boldsymbol{C}_h, \tag{3.3b}$$

where $\bar{\mathbf{B}}_n = \mathbf{curl}\,\bar{\mathbf{A}}_n$. It is well-known that the Crank-Nicolson scheme is of second order with respect to τ.

The discrete problem is nonlinear and expensive to solve at each time step. Thus, inspired by Refs. [3, 37], we resort to the linearly extrapolated solutions

$$\mathbf{u}_n^* = \frac{1}{2}(3\mathbf{u}_{n-1} - \mathbf{u}_{n-2}), \ \ \mathbf{B}_n^* = \frac{1}{2}(3\mathbf{B}_{n-1} - \mathbf{B}_{n-2}) = \frac{1}{2}\,\mathbf{curl}(3\mathbf{A}_{n-1} - \mathbf{A}_{n-2}).$$

The truncation errors for the above approximations are of second order. For any smooth function v, let $\bar{v}_n = [v(t_n) + v(t_{n-1})]/2$ and $v_n^* = [3v(t_{n-1}) - v(t_{n-2})]/2$. It is easy to see

$$v_n^* - \bar{v}_n = \frac{1}{2}[v(t_{n-2}) + v(t_n) - 2v(t_{n-1})] = v_{tt}(t_{n-1})\tau^2 + O(\tau^3). \tag{3.4}$$

For $n = 1$, we define $\mathbf{u}_1^* = \mathbf{u}_0$ and $\mathbf{B}_1^* = \mathbf{curl}\,\mathbf{A}_0$. We linearize the nonlinear terms in (3.3) by replacing $\bar{\mathbf{u}}_n, \bar{\mathbf{B}}_n$ with $\mathbf{u}_n^*$ and $\mathbf{B}_n^*$ respectively. We arrive at the semi-implicit time-stepping scheme for (2.6):

Find $(\mathbf{u}_n, \mathbf{A}_n) \in \boldsymbol{V}_h(\operatorname{div} 0) \times \boldsymbol{C}_h$, $n \geq 1$, such that

$$(\delta_t \mathbf{u}_n, \boldsymbol{v}) + \mathcal{O}_h(\mathbf{u}_n^*; \bar{\mathbf{u}}_n, \boldsymbol{v}) + \mathcal{A}_h(\bar{\mathbf{u}}_n, \boldsymbol{v}) + \kappa(\delta_t \mathbf{A}_n + \mathbf{B}_n^* \times \bar{\mathbf{u}}_n, \mathbf{B}_n^* \times \boldsymbol{v}) = (\boldsymbol{f}_n, \boldsymbol{v}) \quad \forall \boldsymbol{v} \in \boldsymbol{V}_h(\operatorname{div} 0), \tag{3.5a}$$

$$(\delta_t \mathbf{A}_n + \mathbf{B}_n^* \times \bar{\mathbf{u}}_n, \boldsymbol{c}) + \frac{1}{R_m}(\mathbf{curl}\,\bar{\mathbf{A}}_n, \mathbf{curl}\,\boldsymbol{c}) = 0 \qquad \forall \boldsymbol{c} \in \boldsymbol{C}_h. \tag{3.5b}$$

Theorem 3.1. *The discrete problem* (3.5) *has a unique solution in each time step. The discrete energy law*

$$\frac{\mathsf{E}_n - \mathsf{E}_{n-1}}{\tau} + \mathsf{P}_n = (\boldsymbol{f}_n, \bar{\mathbf{u}}_n) \qquad \forall n \geq 1, \tag{3.6}$$

holds, where

$$\mathsf{E}_n := \frac{1}{2}\|\mathbf{u}_n\|_{\boldsymbol{L}^2(\Omega)}^2 + \frac{\kappa}{2R_m}\|\mathbf{curl}\,\mathbf{A}_n\|_{\boldsymbol{L}^2(\Omega)}^2,$$

$$\mathsf{P}_n := \|\bar{\mathbf{u}}_n\|_{\mathcal{A}_h}^2 + \frac{1}{2}\sum_{F \in \mathcal{F}_h}\int_F |\mathbf{u}_n^* \cdot \boldsymbol{n}|\,|[\![\bar{\mathbf{u}}_n]\!]|^2 + \kappa\|\delta_t \mathbf{A}_n + \mathbf{B}_n^* \times \bar{\mathbf{u}}_n\|_{\boldsymbol{L}^2(\Omega)}^2.$$

Proof. We first prove the discrete energy law. Let $\mathbf{J}_n := -\delta_t \mathbf{A}_n - \mathbf{B}_n^* \times \bar{\mathbf{u}}_n$ be the discrete electric current density. Taking $\boldsymbol{v} = \bar{\mathbf{u}}_n$ in (3.5a) yields

$$(\delta_t \mathbf{u}_n, \bar{\mathbf{u}}_n) + \mathcal{O}_h(\mathbf{u}_n^*; \bar{\mathbf{u}}_n, \bar{\mathbf{u}}_n) + \mathcal{A}_h(\bar{\mathbf{u}}_n, \bar{\mathbf{u}}_n) = \kappa(\mathbf{J}_n, \mathbf{B}_n^* \times \bar{\mathbf{u}}_n) + (\boldsymbol{f}_n, \bar{\mathbf{u}}_n). \tag{3.7}$$

Since $\mathbf{u}_n^* \in \boldsymbol{V}_h(\operatorname{div} 0)$, from Lemma 3.3 we have

$$\mathcal{O}_h(\mathbf{u}_n^*; \bar{\mathbf{u}}_n, \bar{\mathbf{u}}_n) = \frac{1}{2}\sum_{F \in \mathcal{F}_h}\int_F |\mathbf{u}_n^* \cdot \boldsymbol{n}|\,|[\![\bar{\mathbf{u}}_n]\!]|^2 .$$

Furthermore, by taking $\boldsymbol{c} = \delta_t \mathbf{A}_n$ in (3.5b), we find that

$$\frac{1}{R_m}\left(\mathbf{curl}\,\bar{\mathbf{A}}_n, \mathbf{curl}\,\delta_t \mathbf{A}_n\right) = (\mathbf{J}_n, \delta_t \mathbf{A}_n) = -(\mathbf{J}_n, \mathbf{B}_n^* \times \bar{\mathbf{u}}_n) - \kappa^{-1}\|\mathbf{J}_n\|_{\boldsymbol{L}^2(\Omega)}^2.$$

It follows that

$$(\mathbf{J}_n, \mathbf{B}_n^* \times \bar{\mathbf{u}}_n) = -\kappa^{-1}\|\mathbf{J}_n\|_{\boldsymbol{L}^2(\Omega)}^2 - \frac{1}{R_m}\left(\mathbf{curl}\,\bar{\mathbf{A}}_n, \mathbf{curl}\,\delta_t \mathbf{A}_n\right). \tag{3.8}$$

By direct calculations, we obtain the identities

$$(\delta_t \mathbf{u}_n, \bar{\mathbf{u}}_n) = \frac{1}{2\tau}\left(\|\mathbf{u}_n\|_{\boldsymbol{L}^2(\Omega)}^2 - \|\mathbf{u}_{n-1}\|_{\boldsymbol{L}^2(\Omega)}^2\right),$$

$$\left(\mathbf{curl}\,\bar{\mathbf{A}}_n, \mathbf{curl}\,\delta_t \mathbf{A}_n\right) = \frac{1}{2\tau}\left(\|\mathbf{curl}\,\mathbf{A}_n\|_{\boldsymbol{L}^2(\Omega)}^2 - \|\mathbf{curl}\,\mathbf{A}_{n-1}\|_{\boldsymbol{L}^2(\Omega)}^2\right).$$

Inserting (3.8) and the above identities into (3.7) yields (3.6).

To prove the well-posedness of (3.5), we write $\bar{\boldsymbol{\Psi}}_n = (\bar{\mathbf{u}}_n, \bar{\mathbf{A}}_n)$ and consider an equivalent form of (3.5): Find $\bar{\boldsymbol{\Psi}}_n \in \boldsymbol{V}_h(\operatorname{div} 0) \times \boldsymbol{C}_h$ such that

$$a(\bar{\boldsymbol{\Psi}}_n, \boldsymbol{\Phi}) = f(\boldsymbol{\Phi}) \qquad \forall\, \boldsymbol{\Phi} \in \boldsymbol{V}_h(\operatorname{div} 0) \times \boldsymbol{C}_h. \tag{3.9}$$

For any $\boldsymbol{\Psi} = (\boldsymbol{w}, \boldsymbol{a})$, $\boldsymbol{\Phi} = (\boldsymbol{v}, \boldsymbol{c})$ with $\boldsymbol{w}, \boldsymbol{v} \in \boldsymbol{V}_h(\operatorname{div} 0)$ and $\boldsymbol{a}, \boldsymbol{c} \in \boldsymbol{C}_h$, the bilinear form and the right-hand side are defined by

$$\begin{aligned} a(\boldsymbol{\Psi}, \boldsymbol{\Phi}) &:= \frac{2}{\tau}(\boldsymbol{w}, \boldsymbol{v}) + \mathcal{O}_h(\mathbf{u}_n^*; \boldsymbol{w}, \boldsymbol{v}) + \mathcal{A}_h(\boldsymbol{w}, \boldsymbol{v}) + \frac{2\kappa}{\tau R_m}(\mathbf{curl}\, \boldsymbol{a}, \mathbf{curl}\, \boldsymbol{c}) \\ &\quad + \kappa\left(\frac{2}{\tau}\boldsymbol{a} + \mathbf{B}_n^* \times \boldsymbol{w}, \frac{2}{\tau}\boldsymbol{c} + \mathbf{B}_n^* \times \boldsymbol{v}\right), \\ f(\boldsymbol{\Phi}) &:= \left(\boldsymbol{f}_n + \frac{2}{\tau}\mathbf{u}_{n-1}, \boldsymbol{v}\right) + \kappa\left(\frac{2}{\tau}\mathbf{A}_{n-1}, \frac{2}{\tau}\boldsymbol{c} + \mathbf{B}_n^* \times \boldsymbol{v}\right). \end{aligned} \tag{3.10}$$

It is easy to see that

$$|||\boldsymbol{\Phi}||| = \left(\frac{2}{\tau}\|\boldsymbol{v}\|^2_{\boldsymbol{L}^2(\Omega)} + \|\boldsymbol{v}\|^2_{\mathcal{A}_h} + \frac{2\kappa}{\tau R_m}\|\mathbf{curl}\, \boldsymbol{c}\|^2_{\boldsymbol{L}^2(\Omega)} + \kappa\left\|\frac{2}{\tau}\boldsymbol{c} + \mathbf{B}_n^* \times \boldsymbol{v}\right\|^2_{\boldsymbol{L}^2(\Omega)}\right)^{\frac{1}{2}}$$

provides a norm on $\boldsymbol{V}_h(\operatorname{div} 0) \times \boldsymbol{C}_h$. From Lemma 3.3, $\mathcal{O}_h\big(\mathbf{u}_n^*; \boldsymbol{v}, \boldsymbol{v}\big) \geq 0$ and

$$a(\boldsymbol{\Phi}, \boldsymbol{\Phi}) \geq |||\boldsymbol{\Phi}|||^2 \qquad \forall\, \boldsymbol{\Phi} \in \boldsymbol{V}_h(\operatorname{div} 0) \times \boldsymbol{C}_h\ .$$

Therefore, the bilinear form $a(\cdot, \cdot)$ is coercive on $\boldsymbol{V}_h(\operatorname{div} 0) \times \boldsymbol{C}_h$.

By Schwarz's inequality, we find that

$$|a(\boldsymbol{\Psi}, \boldsymbol{\Phi})| \leq |||\boldsymbol{\Psi}|||\ |||\boldsymbol{\Phi}||| + |\mathcal{O}_h(\mathbf{u}_*; \boldsymbol{w}, \boldsymbol{v})|\,.$$

From Lemma 3.3 and Lemma 3.2, we have

$$|\mathcal{O}_h(\mathbf{u}_n^*; \boldsymbol{w}, \boldsymbol{v})| \leq C_0\|\mathbf{u}_n^*\|_{1,h}\|\boldsymbol{w}\|_{1,h}\|\boldsymbol{v}\|_{1,h} \leq C_0\theta_1^2 R_e^{-2}\|\mathbf{u}_n^*\|_{1,h}\|\boldsymbol{w}\|_{\mathcal{A}_h}\|\boldsymbol{v}\|_{\mathcal{A}_h}\,.$$

This implies the continuity of $a(\cdot, \cdot)$, namely,

$$|a(\boldsymbol{\Psi}, \boldsymbol{\Phi})| \leq \left(1 + C_0\theta_1^2 R_e^{-2}\|\mathbf{u}_n^*\|_{1,h}\right)|||\boldsymbol{\Psi}|||\ |||\boldsymbol{\Phi}|||\,.$$

By the Lax-Milgram lemma, the linear problem (3.9) has a unique solution. □

Remark 3.1. The discrete energy law can be understood similarly as in Remark 2.1. For the discrete scheme, the tangential discontinuity of the velocity also introduces a dissipative term due to the upwind flux.

Corollary 3.1. *There exists a constant $C > 0$ depending only on physical parameters such that*

$$\mathsf{E}_m + \frac{1}{2}\sum_{n=1}^{m}\tau\mathsf{P}_n \leq \mathsf{E}_0 + C\sum_{n=1}^{m}\tau\|\boldsymbol{f}_n\|^2_{\boldsymbol{L}^2(\Omega)}\,, \quad 1 \leq m \leq N.$$

Proof. From Theorem 3.1 we know that

$$\frac{\mathsf{E}_n - \mathsf{E}_{n-1}}{\tau} + \mathsf{P}_n = (\boldsymbol{f}_n, \bar{\mathbf{u}}_n) \qquad \forall\, n \geq 1.$$

Summing the above equality with respect to $n = 1, \cdots, m$, we have

$$\mathsf{E}_m + \sum_{n=1}^{m} \tau \mathsf{P}_n = \mathsf{E}_0 + \sum_{n=1}^{m} \tau(\boldsymbol{f}_n, \bar{\mathbf{u}}_n). \tag{3.11}$$

Similarly, by Lemma 3.1 and Lemma 3.2, we have

$$\begin{aligned} |(\boldsymbol{f}_n, \bar{\mathbf{u}}_n)| &\leq \|\boldsymbol{f}_n\|_{\boldsymbol{L}^2(\Omega)} \|\bar{\mathbf{u}}_n\|_{\boldsymbol{L}^2(\Omega)} \leq C \|\boldsymbol{f}_n\|_{\boldsymbol{L}^2(\Omega)} \|\bar{\mathbf{u}}_n\|_{\mathcal{A}_h} \\ &\leq C \|\boldsymbol{f}_n\|_{\boldsymbol{L}^2(\Omega)}^2 + \frac{1}{2} \|\bar{\mathbf{u}}_n\|_{\mathcal{A}_h}^2 . \end{aligned}$$

Summing all the equalities with respect to $n = 1, \cdots, m$ yields

$$\sum_{n=1}^{m} \tau(\boldsymbol{f}_n, \bar{\mathbf{u}}_n) \leq C \sum_{n=1}^{m} \tau \|\boldsymbol{f}_n\|_{\boldsymbol{L}^2(\Omega)}^2 + \frac{1}{2} \sum_{n=1}^{m} \tau \mathsf{P}_n. \tag{3.12}$$

The proof is completed by inserting (3.12) into (3.11). □

4. Convergence of discrete solutions

The purpose of this section is to prove the convergence of discrete solutions as $h, \tau \to 0$. For simplicity, we shall first fix the timestep τ and let the meshwidth h tend to zero. This will yield a semi-discrete model of the MHD equations. Next we shall let $\tau \to 0$ and prove the convergence of the semi-discrete solutions. Since we only use the stability of discrete solutions in (3.1) without any additional assumptions, the convergence of discrete solutions is obtained only for an extracted subsequence instead of the whole sequence $(\mathbf{u}_n, \mathbf{A}_n)$. The idea of this part is borrowed from [30] where the $\boldsymbol{B}$-based MHD formulation is studied and the velocity $\boldsymbol{u}$ is discretized by continuous finite elements.

Without loss of generality, let $\mathcal{T}_1 \prec \mathcal{T}_2 \prec \cdots \prec \mathcal{T}_k \prec \cdots$ be a quasi-uniform and shape-regular sequence of meshes of Ω such that $\lim_{k\to\infty} h_k = 0$ and $\mathcal{T}_{k+1}$ is a refinement of $\mathcal{T}_k$. To specify the dependency of discrete solutions on $\mathcal{T}_k$, we endow them with a superscript and write $\mathbf{u}_n^{(k)} := \mathbf{u}_n$, $\mathbf{B}_n^{(k)} := \mathbf{B}_n$, and $\mathbf{A}_n^{(k)} := \mathbf{A}_n$. Without specifications, $\|\boldsymbol{v}_k\|_{1,h}$ will denote the discrete norm of $\boldsymbol{v}_k \in \boldsymbol{D}_m(\mathcal{T}_k)$ on the mesh $\mathcal{T}_k$. The same principle also applies to $|\cdot|_{1,h}$, $\mathcal{A}_h$, $\mathcal{O}_h$ etc. Throughout this section, in the case of sequences such as $\mathbf{u}_n^{(k)}$ and $\mathbf{A}_n^{(k)}$, we retain the same notation even after extracting subsequences.

Theorem 4.1. *There are subsequences of discrete solutions* $\left\{\left(\mathbf{u}_n^{(k)}, \mathbf{A}_n^{(k)}\right)\right\}_{k=1}^{\infty}$ *and a pair of functions* $(\boldsymbol{u}_n, \boldsymbol{A}_n) \in \boldsymbol{V}(\operatorname{div} 0) \times \boldsymbol{C}$ *such that for* $k \to \infty$

$$\begin{aligned} &\mathbf{u}_n^{(k)} \to \boldsymbol{u}_n && \textit{strongly in } \boldsymbol{L}^4(\Omega), \\ &\mathbf{A}_n^{(k)} \rightharpoonup \boldsymbol{A}_n && \textit{weakly in } \boldsymbol{L}^{3/2}(\Omega), \\ &\mathbf{B}_n^{(k)} \to \boldsymbol{B}_n = \mathbf{curl}\, \boldsymbol{A}_n && \textit{strongly in } \boldsymbol{L}^2(\Omega), \end{aligned}$$

Moreover, the limits satisfy, for any $(\boldsymbol{v}, \boldsymbol{c}) \in \boldsymbol{V}(\operatorname{div} 0) \times \boldsymbol{C}$,

$$\begin{aligned} &(\delta_t \boldsymbol{u}_n, \boldsymbol{v}) + \mathcal{O}(\boldsymbol{u}_n^*; \bar{\boldsymbol{u}}_n, \boldsymbol{v}) + \mathcal{A}(\bar{\boldsymbol{u}}_n, \boldsymbol{v}) - \kappa\, (\delta_t \boldsymbol{A}_n + \boldsymbol{B}_n^* \times \bar{\boldsymbol{u}}_n, \boldsymbol{B}_n^* \times \boldsymbol{v}) = (\boldsymbol{f}_n, \boldsymbol{v}), \\ &(\delta_t \boldsymbol{A}_n + \boldsymbol{B}_n^* \times \bar{\boldsymbol{u}}_n, \boldsymbol{c}) + R_m^{-1} \left(\mathbf{curl}\, \bar{\boldsymbol{A}}_n, \mathbf{curl}\, \boldsymbol{c}\right) = 0, \end{aligned}$$

where

$$\begin{aligned} \bar{\boldsymbol{u}}_n &= (\boldsymbol{u}_n + \boldsymbol{u}_{n-1})/2, & \boldsymbol{u}_n^* &= (3\boldsymbol{u}_{n-1} - \boldsymbol{u}_{n-2})/2, \\ \bar{\boldsymbol{A}}_n &= (\boldsymbol{A}_n + \boldsymbol{A}_{n-1})/2, & \boldsymbol{B}_n^* &= (3\boldsymbol{B}_{n-1} - \boldsymbol{B}_{n-2})/2. \end{aligned}$$

Next, to study the convergence of $\boldsymbol{u}_n, \boldsymbol{A}_n$ as $\tau \to 0$, we define interpolants of semi-discrete functions in time by

$$\begin{cases} \boldsymbol{u}_\tau(t) = l(t)\boldsymbol{u}_{n-1} + [1 - l(t)]\boldsymbol{u}_n, \\ \boldsymbol{A}_\tau(t) = l(t)\boldsymbol{A}_{n-1} + [1 - l(t)]\boldsymbol{A}_n, & \forall\, t \in [t_{n-1}, t_n), \\ \boldsymbol{f}_\tau(t) = \boldsymbol{f}_n, \end{cases}$$

where $l(t) = (t_n - t)/\tau$ and $1 \le n \le N$. Now we can state the main theorem of this section.

Theorem 4.2. *Assume* $\lim_{\tau \to 0} \|\boldsymbol{f}_\tau - \boldsymbol{f}\|_{\boldsymbol{L}^2(0,T;\boldsymbol{L}^2(\Omega))} = 0$. *Then there is a subsequence of semi-discrete solutions* $(\boldsymbol{u}_\tau, \boldsymbol{A}_\tau)$ *such that*

$$\begin{aligned} &\boldsymbol{u}_\tau \rightharpoonup \boldsymbol{u} && \textit{weakly in } \boldsymbol{L}^2(0, T; \boldsymbol{V}(\operatorname{div} 0)), \\ &\boldsymbol{A}_\tau \rightharpoonup \boldsymbol{A} && \textit{weakly in } \boldsymbol{W}^{1,r}(0, T; \boldsymbol{C}). \end{aligned}$$

Moreover, the limits $(\boldsymbol{u}, \boldsymbol{A})$ *are solutions to problem* (2.6).

The main purpose of this section is to prove Theorem 4.1 and Theorem 4.2. Their proofs will be elaborated in Subsection 4.1 and Subsection 4.2 respectively.

Remark 4.1. Theorem 4.2, actually proves the existence of weak solutions to the continuous problem (2.6). Since we are only interested in numerical solutions, the uniqueness of solutions is very difficult for general initial values and right-hand sides and is beyond the scope of this paper. We refer to [14] for the discussions of the $\boldsymbol{B}$-based MHD formulation.

4.1. *Proof of Theorem 4.1*

The proof of Theorem 4.1 will be given at the end of this subsection. We start by introducing the subspaces

$$\boldsymbol{X}_t := \boldsymbol{H}(\mathbf{curl}, \Omega) \cap \boldsymbol{H}_0(\mathrm{div}, \Omega), \qquad \boldsymbol{X}_n := \boldsymbol{H}_0(\mathbf{curl}, \Omega) \cap \boldsymbol{H}(\mathrm{div}, \Omega),$$

which are equipped with the following norm

$$\|\boldsymbol{v}\|_{\boldsymbol{X}_t} = \|\boldsymbol{v}\|_{\boldsymbol{X}_n} = \left(\|\mathbf{curl}\, \boldsymbol{v}\|^2_{\boldsymbol{L}^2(\Omega)} + \|\mathrm{div}\, \boldsymbol{v}\|^2_{L^2(\Omega)}\right)^{1/2}.$$

Clearly $\boldsymbol{C}(\mathrm{div}\, 0) := \boldsymbol{H}_0(\mathbf{curl}, \Omega) \cap \boldsymbol{H}(\mathrm{div}\, 0, \Omega) \subset \boldsymbol{X}_n$. By Theorem 3.50 of Ref. [25], we have the compact injections with a constant $s > 1/2$ depending only on Ω

$$\boldsymbol{X}_t \hookrightarrow\hookrightarrow \boldsymbol{H}^s(\Omega), \qquad \boldsymbol{X}_n \hookrightarrow\hookrightarrow \boldsymbol{H}^s(\Omega), \tag{4.1}$$

and for any $\boldsymbol{v} \in \boldsymbol{X}_t$ or $\boldsymbol{v} \in \boldsymbol{X}_n$,

$$\|\boldsymbol{v}\|_{\boldsymbol{H}^s(\Omega)} \le C \left(\|\mathbf{curl}\, \boldsymbol{v}\|_{\boldsymbol{L}^2(\Omega)} + \|\mathrm{div}\, \boldsymbol{v}\|_{L^2(\Omega)}\right). \tag{4.2}$$

Let $\boldsymbol{V}_k$, $\boldsymbol{V}_k(\mathrm{div}\, 0)$, $\boldsymbol{C}_k$ denote the finite element spaces $\boldsymbol{V}_h$, $\boldsymbol{V}_h(\mathrm{div}\, 0)$, and $\boldsymbol{C}_h$ on $\mathcal{T}_k$ respectively. In addition we write

$$L_m(\mathcal{T}_h) := \{v \in H^1(\Omega) : v|_K \in P_m(K), K \in \mathcal{T}_h\}$$

for the **L**agrangian finite element space of polynomial degree m. The weakly divergence-free subspace of $\boldsymbol{C}_k$ is defined by

$$\boldsymbol{C}_k(\mathrm{div}\, 0) := \left\{\boldsymbol{w}_h \in \boldsymbol{C}_k :\ (\boldsymbol{w}_h, \nabla v_h) = 0,\ \ \forall\, v_h \in L_2(\mathcal{T}_k) \cap H^1_0(\Omega)\right\}.$$

Since we assume that the boundary of Ω is connected, by the discrete Poincaré-Friedrichs inequality [19, Theorem 4.7], there is a constant $C > 0$ depending only on Ω and the shape regularity of $\mathcal{T}_k$ such that

$$\|\boldsymbol{w}_h\|_{\boldsymbol{L}^2(\Omega)} \le C\, \|\mathbf{curl}\, \boldsymbol{w}_h\|_{\boldsymbol{L}^2(\Omega)} \qquad \forall\, \boldsymbol{w}_h \in \boldsymbol{C}_k(\mathrm{div}\, 0). \tag{4.3}$$

Let $\mathcal{P}$: $\boldsymbol{L}^2(\Omega) \to \nabla H^1_0(\Omega)$ and $\mathcal{P}_k$: $\boldsymbol{L}^2(\Omega) \to \nabla\left[L_2(\mathcal{T}_k) \cap H^1_0(\Omega)\right]$ be the $L^2(\Omega)$-orthogonal projections and define $\mathcal{Q} := \mathcal{I} - \mathcal{P}$, $\mathcal{Q}_k := \mathcal{I} - \mathcal{P}_k$. Obviously, we have

$$\mathcal{Q}(\boldsymbol{C}) = \boldsymbol{C}(\mathrm{div}\, 0), \qquad \mathcal{Q}_k(\boldsymbol{C}_k) = \boldsymbol{C}_k(\mathrm{div}\, 0).$$

Let $\mathbf{a}_n^{(k)} := \mathcal{Q}_k\big(\mathbf{A}_n^{(k)}\big)$ be the weakly divergence-free component of $\mathbf{A}_n^{(k)}$. Then

$$\mathbf{B}_n^{(k)} = \mathbf{curl}\, \mathbf{A}_n^{(k)} = \mathbf{curl}\, \mathbf{a}_n^{(k)}.$$

Since $\boldsymbol{A}_0 \in \boldsymbol{C}(\mathrm{div}\, 0)$, we assume $\mathbf{A}_0^{(k)} = \mathbf{a}_0^{(k)} \in \boldsymbol{C}_k(\mathrm{div}\, 0)$ without loss of generality.

Lemma 4.1. *Suppose the initial conditions satisfy* $\lim\limits_{k\to\infty} \left\|\mathbf{a}_0^{(k)} - \boldsymbol{A}_0\right\|_{\boldsymbol{H}(\mathbf{curl},\Omega)} = 0.$

(1) *There are functions* $(\boldsymbol{u}_n, \boldsymbol{a}_n) \in \boldsymbol{V}(\operatorname{div} 0) \times \boldsymbol{C}(\operatorname{div} 0)$ *and a subsequence of* $\big(\mathbf{u}_n^{(k)}, \mathbf{a}_n^{(k)}\big)$ *such that, as* $k \to \infty$,

$$\begin{aligned} &\mathbf{u}_n^{(k)} \to \boldsymbol{u}_n \quad \textit{strongly in } \boldsymbol{L}^4(\Omega), \\ &\mathbf{a}_n^{(k)} \to \boldsymbol{a}_n \quad \textit{strongly in } \boldsymbol{C}, \\ &\mathbf{J}_n^{(k)} \rightharpoonup \boldsymbol{J}_n = -\delta_t \boldsymbol{a}_n - \mathcal{Q}(\boldsymbol{B}_n^* \times \bar{\boldsymbol{u}}_n) \quad \textit{weakly in } \boldsymbol{L}^2(\Omega), \end{aligned}$$

where $\boldsymbol{B}_n^* = (3\boldsymbol{B}_{n-1} - \boldsymbol{B}_{n-2})/2$ *and* $\boldsymbol{B}_n = \mathbf{curl}\, \boldsymbol{a}_n$.

(2) *Write* $\bar{\boldsymbol{a}}_n = (\boldsymbol{a}_n + \boldsymbol{a}_{n-1})/2$. *The limits satisfy the weak formulation*

$$R_m\,(\boldsymbol{J}_n, \boldsymbol{c}) + (\mathbf{curl}\, \bar{\boldsymbol{a}}_n, \mathbf{curl}\, \boldsymbol{c}) = 0 \quad \forall\, \boldsymbol{c} \in \boldsymbol{C}. \tag{4.4}$$

Lemma 4.2. *Let* $\boldsymbol{u}_n, \boldsymbol{B}_n, \boldsymbol{J}_n$ *be the limits of* $\mathbf{u}_n^{(k)}$, $\mathbf{B}_n^{(k)}$, $\mathbf{J}_n^{(k)}$ *and define* $\boldsymbol{u}_n^* = (3\boldsymbol{u}_{n-1} - \boldsymbol{u}_{n-2})/2$. *Then for any* $\boldsymbol{v} \in \boldsymbol{V}(\operatorname{div} 0)$,

$$(\delta_t \boldsymbol{u}_n, \boldsymbol{v}) + \mathcal{O}(\boldsymbol{u}_n^*; \bar{\boldsymbol{u}}_n, \boldsymbol{v}) + \mathcal{A}(\bar{\boldsymbol{u}}_n, \boldsymbol{v}) - \kappa\,(\boldsymbol{J}_n, \boldsymbol{B}_n^* \times \boldsymbol{v}) = (\boldsymbol{f}_n, \boldsymbol{v}). \tag{4.5}$$

The proofs of Lemma 4.1 and Lemma 4.2 are given in Appendix B. Now we are in a position to prove Theorem 4.1.

Proof of Theorem 4.1. By Schwarz's inequality and Lemma 3.1, we have

$$\left\|\mathbf{B}_n^{*(k)} \times \bar{\mathbf{u}}_n^{(k)}\right\|_{\boldsymbol{L}^{3/2}(\Omega)} \leq \left\|\mathbf{B}_n^{*(k)}\right\|_{\boldsymbol{L}^2(\Omega)} \left\|\bar{\mathbf{u}}_n^{(k)}\right\|_{\boldsymbol{L}^6(\Omega)} \leq \left\|\mathbf{B}_n^{*(k)}\right\|_{\boldsymbol{L}^2(\Omega)} \left\|\bar{\mathbf{u}}_n^{(k)}\right\|_{1,h} \leq C.$$

There exists a subsequence such that

$$\mathbf{B}_n^{*(k)} \times \bar{\mathbf{u}}_n^{(k)} \rightharpoonup \boldsymbol{B}_n \times \boldsymbol{u}_n \quad \text{weakly in } \boldsymbol{L}^{3/2}(\Omega).$$

The boundedness of $\mathbf{J}_n^{(k)}$ implies that $\delta_t \mathbf{A}_n^{(k)}$ are also bounded in $\boldsymbol{L}^{3/2}(\Omega)$. Consider the $L^2(\Omega)$-orthogonal decomposition

$$\mathbf{A}_n^{(k)} = \mathbf{a}_n^{(k)} + \nabla \psi_n^{(k)}, \quad \psi_n^{(k)} \in L_2(\mathcal{T}_k) \cap H_0^1(\Omega).$$

By Lemma 4.1, $\mathbf{a}_n^{(k)}$ converges strongly to $\boldsymbol{a}_n$ in $\boldsymbol{C}$. We find that

$$\psi_n^{(k)} \rightharpoonup \psi_n \quad \text{weakly in } W_0^{1,3/2}(\Omega).$$

Collecting these facts yields

$$\boldsymbol{J}_n = -\delta_t(\boldsymbol{a}_n + \nabla \psi_n) - \boldsymbol{B}_n^* \times \boldsymbol{u}_n.$$

Since $\boldsymbol{B}_n^* \times \boldsymbol{u}_n \in \boldsymbol{L}^2(\Omega)$ by (B.10), we also have $\boldsymbol{A}_n := \boldsymbol{a}_n + \nabla \psi_n \in \boldsymbol{L}^2(\Omega)$. Then (4.4) implies

$$(\delta_t \boldsymbol{A}_n + \boldsymbol{B}_n^* \times \bar{\boldsymbol{u}}_n, \boldsymbol{c}) + \frac{1}{R_m}\big(\mathbf{curl}\, \bar{\boldsymbol{A}}_n, \mathbf{curl}\, \boldsymbol{c}\big) = 0 \qquad \forall\, \boldsymbol{c} \in \boldsymbol{C}.$$

Then Theorem 4.1 follows from the above equation and (4.5). $\square$

4.2. *Proof of Theorem 4.2*

The proof of Theorem 4.2 will be given at the end of this subsection. For convenience, we define the piecewise linear interpolant of $\boldsymbol{a}_n$ by

$$\boldsymbol{a}_\tau(t) = l(t)\boldsymbol{a}_{n-1} + [1 - l(t)]\boldsymbol{a}_n \qquad \forall\, t \in [t_{n-1}, t_n).$$

Define piecewise constant functions in the time variable by

$$\bar{\boldsymbol{u}}_\tau(t) = \bar{\boldsymbol{u}}_n, \quad \bar{\boldsymbol{a}}_\tau(t) = \bar{\boldsymbol{a}}_n, \quad \boldsymbol{u}^*_\tau(t) = \boldsymbol{u}^*_n, \quad \boldsymbol{B}^*_\tau(t) = \boldsymbol{B}^*_n \qquad \forall\, t \in [t_{n-1}, t_n).$$

Moreover, we shall also use the interpolated magnetic inductions and current density

$$\boldsymbol{B}_\tau = \mathbf{curl}\,\boldsymbol{a}_\tau, \quad \bar{\boldsymbol{B}}_\tau = \mathbf{curl}\,\bar{\boldsymbol{a}}_\tau, \quad \boldsymbol{J}_\tau = -\partial_t \boldsymbol{a}_\tau - \mathcal{Q}(\boldsymbol{B}^*_\tau \times \bar{\boldsymbol{u}}_\tau).$$

From (4.4) and (4.5), we know that $(\boldsymbol{u}_\tau, \boldsymbol{a}_\tau)$ satisfy

$$(\partial_t \boldsymbol{u}_\tau, \boldsymbol{v}) + \mathcal{O}(\boldsymbol{u}^*_\tau; \bar{\boldsymbol{u}}_\tau, \boldsymbol{v}) + \mathcal{A}(\bar{\boldsymbol{u}}_\tau, \boldsymbol{v}) - \kappa\,(\boldsymbol{J}_\tau, \boldsymbol{B}^*_\tau \times \boldsymbol{v}) = (\boldsymbol{f}_\tau, \boldsymbol{v}), \tag{4.6a}$$

$$R_m\,(\boldsymbol{J}_\tau, \boldsymbol{c}) + (\mathbf{curl}\,\bar{\boldsymbol{a}}_\tau, \mathbf{curl}\,\boldsymbol{c}) = 0, \tag{4.6b}$$

for all $\boldsymbol{v} \in \boldsymbol{V}(\mathrm{div}\,0)$ and $\boldsymbol{c} \in \boldsymbol{C}(\mathrm{div}\,0)$.

Lemma 4.3. *Let $s > 1/2$ be the constant in* (4.1) *and define $r = 8s/(2s+3) > 1$. There is a constant $C > 0$ independent of τ such that for all timesteps τ*

$$\|\boldsymbol{u}_\tau\|_{\boldsymbol{L}^\infty(0,T;\boldsymbol{L}^2(\Omega))} + \|\bar{\boldsymbol{u}}_\tau\|_{\boldsymbol{L}^2(0,T;\boldsymbol{H}^1(\Omega))} \le C, \tag{4.7}$$

$$\|\boldsymbol{a}_\tau\|_{\boldsymbol{L}^\infty(0,T;\boldsymbol{X}_n)} + \|\boldsymbol{B}_\tau\|_{\boldsymbol{L}^2(0,T;\boldsymbol{X}_t)} + \|\boldsymbol{J}_\tau\|_{\boldsymbol{L}^2(0,T;\boldsymbol{L}^2(\Omega))} \le C, \tag{4.8}$$

$$\|\partial_t \boldsymbol{a}_\tau\|_{\boldsymbol{L}^r(0,T;\boldsymbol{L}^2(\Omega))} + \|\boldsymbol{B}^*_\tau \times \bar{\boldsymbol{u}}_\tau\|_{\boldsymbol{L}^r(0,T;\boldsymbol{L}^2(\Omega))} \le C. \tag{4.9}$$

Proof. By the assumption of Theorem 4.2, $\{\boldsymbol{f}_\tau\}$ is bounded in $\boldsymbol{L}^2(0,T;\boldsymbol{L}^2(\Omega))$. By arguments similar to the proof of Theorem 2.1, we obtain (4.7) and

$$\|\boldsymbol{B}_\tau\|_{\boldsymbol{L}^\infty(0,T;\boldsymbol{L}^2(\Omega))} + \|\boldsymbol{J}_\tau\|^2_{\boldsymbol{L}^2(0,T;\boldsymbol{L}^2(\Omega))} \le C.$$

Since $\mathrm{div}\,\boldsymbol{a}_\tau = 0$, we have

$$\|\boldsymbol{a}_\tau\|_{\boldsymbol{L}^\infty(0,T;\boldsymbol{X}_n)} \le C\,\|\mathbf{curl}\,\boldsymbol{a}_\tau\|_{\boldsymbol{L}^\infty(0,T;\boldsymbol{L}^2(\Omega))} \le C.$$

Similarly, since $\mathrm{div}\,\boldsymbol{B}_\tau = 0$, we have

$$\|\boldsymbol{B}_\tau\|_{\boldsymbol{L}^2(0,T;\boldsymbol{X}_t)} \le C\,\|\mathbf{curl}\,\boldsymbol{B}_\tau\|_{\boldsymbol{L}^2(0,T;\boldsymbol{L}^2(\Omega))} \le C\,\|\boldsymbol{J}_\tau\|_{\boldsymbol{L}^2(0,T;\boldsymbol{L}^2(\Omega))} \le C.$$

From (B.9) of Appendix B, we have $\boldsymbol{B}^*_n \in \boldsymbol{L}^q(\Omega)$ for $q = 6/(3-2s) > 3$, that is, $\boldsymbol{B}^*_\tau \in \boldsymbol{L}^q(\Omega)$. Note that $r = 2(q-2)/(q-1)$ and $r' := r/(r-1) = 2(q-2)/(q-3)$. For any $\boldsymbol{v} \in \boldsymbol{L}^{r'}(0,T;\boldsymbol{L}^2(\Omega))$, using Lemma 4.3 and Schwarz's inequality, we have

$$\begin{aligned}
\int_0^T |(\boldsymbol{B}^*_\tau \times \bar{\boldsymbol{u}}_\tau, \boldsymbol{v})| &\le \int_0^T \|\boldsymbol{B}^*_\tau\|_{\boldsymbol{L}^3(\Omega)}\,\|\bar{\boldsymbol{u}}_\tau\|_{\boldsymbol{L}^6(\Omega)}\,\|\boldsymbol{v}\|_{\boldsymbol{L}^2(\Omega)} \\
&\le C\int_0^T \|\boldsymbol{B}^*_\tau\|^{(q-3)/(q-2)}_{\boldsymbol{L}^2(\Omega)}\,\|\boldsymbol{B}^*_\tau\|^{1/(q-2)}_{\boldsymbol{L}^q(\Omega)}\,\|\bar{\boldsymbol{u}}_\tau\|_{\boldsymbol{H}^1(\Omega)}\,\|\boldsymbol{v}\|_{\boldsymbol{L}^2(\Omega)} \\
&\le C\,\|\mathbf{curl}\,\boldsymbol{B}^*_\tau\|^{1/r}_{\boldsymbol{L}^2(0,T;\boldsymbol{L}^2(\Omega))}\,\|\bar{\boldsymbol{u}}_\tau\|_{\boldsymbol{L}^{r'}(0,T;\boldsymbol{H}^1(\Omega))}\,\|\boldsymbol{v}\|_{\boldsymbol{L}^2(0,T;\boldsymbol{L}^2(\Omega))} \\
&\le C\,\|\boldsymbol{v}\|_{\boldsymbol{L}^{r'}(0,T;\boldsymbol{L}^2(\Omega))}\,.
\end{aligned} \tag{4.10}$$

This means that $\boldsymbol{B}_\tau^* \times \bar{\boldsymbol{u}}_\tau$ are uniformly bounded in $\boldsymbol{L}^r(0,T;\boldsymbol{L}^2(\Omega))$. The boundedness of $\partial_t \boldsymbol{a}_\tau$ follows from the boundedness of $\boldsymbol{J}_\tau$ and $\boldsymbol{B}_\tau^* \times \bar{\boldsymbol{u}}_\tau$. □

Now we quote from Lemma 2.8 of Ref. [11] the following lemma on compact injections of Bochner spaces.

Lemma 4.4. *Let B be a Banach space and B_0, B_1 be two reflexive Banach spaces. Assume $B_0 \subset B$ with compact injection and $B \subset B_1$ with continuous injection. Then, for any $1 < p_0, p_1 < +\infty$, the following embedding is compact*

$$\{v \in L^{p_0}(0,T;B_0) : \partial_t v \in L^{p_1}(0,T;B_1)\} \subset L^{p_0}(0,T;B).$$

Lemma 4.5. *There are subsequences of $\boldsymbol{u}_\tau$, $\boldsymbol{a}_\tau$ such that for $\tau \to 0$*

$$\begin{array}{lll}
\boldsymbol{u}_\tau \rightharpoonup \boldsymbol{u} & \textit{weakly} & \textit{in } \boldsymbol{L}^2(0,T;\boldsymbol{V}(\operatorname{div} 0)),\\
\boldsymbol{a}_\tau \rightharpoonup \boldsymbol{a} & \textit{weakly}^* & \textit{in } \boldsymbol{L}^\infty(0,T;\boldsymbol{C}(\operatorname{div} 0)),\\
\boldsymbol{B}_\tau \to \boldsymbol{B} := \mathbf{curl}\, \boldsymbol{a} & \textit{strongly} & \textit{in } \boldsymbol{L}^2(0,T;\boldsymbol{H}^s(\Omega)),\\
\boldsymbol{B}_\tau^* \times \bar{\boldsymbol{u}}_\tau \rightharpoonup \boldsymbol{B} \times \boldsymbol{u} & \textit{weakly} & \textit{in } \boldsymbol{L}^r(0,T;\boldsymbol{L}^2(\Omega)),\\
\boldsymbol{J}_\tau \rightharpoonup \boldsymbol{J} := -\partial_t \boldsymbol{a} - \mathcal{Q}(\boldsymbol{B} \times \boldsymbol{u}) & \textit{weakly} & \textit{in } \boldsymbol{L}^2(0,T;\boldsymbol{L}^2(\Omega)).
\end{array}$$

Moreover, the limits satisfy

$$(\mathbf{curl}\, \boldsymbol{a}, \mathbf{curl}\, \boldsymbol{c}) = R_m(\boldsymbol{J}, \boldsymbol{c}) \qquad \forall\, \boldsymbol{c} \in \boldsymbol{C}. \tag{4.11}$$

Proof. By Lemma 4.3, we can extract subsequences such that for $\tau \to 0$

$$\begin{array}{lll}
\boldsymbol{u}_\tau \rightharpoonup \boldsymbol{u} & \text{weakly} & \text{in } \boldsymbol{L}^2(0,T;\boldsymbol{V}(\operatorname{div} 0)),\\
\boldsymbol{a}_\tau \rightharpoonup \boldsymbol{a} & \text{weakly}^* & \text{in } \boldsymbol{L}^\infty(0,T;\boldsymbol{C}(\operatorname{div} 0)),\\
\boldsymbol{J}_\tau \rightharpoonup \boldsymbol{J} & \text{weakly} & \text{in } \boldsymbol{L}^2(0,T;\boldsymbol{L}^2(\Omega)),\\
\partial_t \boldsymbol{a}_\tau \rightharpoonup \partial_t \boldsymbol{a} & \text{weakly} & \text{in } \boldsymbol{L}^r(0,T;\boldsymbol{L}^2(\Omega)),\\
\boldsymbol{B}_\tau^* \times \bar{\boldsymbol{u}}_\tau \rightharpoonup \boldsymbol{B} \times \boldsymbol{u} & \text{weakly} & \text{in } \boldsymbol{L}^r(0,T;\boldsymbol{L}^2(\Omega)).
\end{array}$$

Therefore, we conclude $\boldsymbol{J} = -\partial_t \boldsymbol{a} - \mathcal{Q}(\boldsymbol{B} \times \boldsymbol{u})$.

From Lemma 4.3, $\partial_t \boldsymbol{a}_\tau$ are uniformly bounded in $\boldsymbol{L}^r(0,T;\boldsymbol{L}^2(\Omega))$. So $\partial_t \boldsymbol{B}_\tau = \mathbf{curl}(\partial_t \boldsymbol{a}_\tau)$ are τ-uniformly bounded in $\boldsymbol{L}^r(0,T;\boldsymbol{C}')$. Since $\boldsymbol{B}_\tau$ is τ-uniformly bounded in $\boldsymbol{L}^2(0,T;\boldsymbol{X}_t)$ and $\boldsymbol{X}_t \hookrightarrow\hookrightarrow \boldsymbol{H}^s(\Omega)$, by Lemma 4.4, we can extract a subsequence of $\boldsymbol{B}_\tau$ which converges strongly to $\boldsymbol{B}$ in $\boldsymbol{L}^2(0,T;\boldsymbol{H}^s(\Omega))$. By passage to $\tau \to 0$ in (4.6b), we obtain equation (4.11) directly from the weak convergence of $\boldsymbol{J}_\tau$ and the strong convergence of $\bar{\boldsymbol{B}}_\tau$. □

Lemma 4.6. *Let r be given in Lemma 4.3 and $(\boldsymbol{u}, \boldsymbol{a})$ be the limits of $(\boldsymbol{u}_\tau, \boldsymbol{a}_\tau)$. Then $\partial_t \boldsymbol{u} \in \boldsymbol{L}^r(0,T;\boldsymbol{V}(\operatorname{div} 0)')$ and*

$$(\partial_t \boldsymbol{u}, \boldsymbol{v}) + \mathcal{O}(\boldsymbol{u}; \boldsymbol{u}, \boldsymbol{v}) + \mathcal{A}(\boldsymbol{u}, \boldsymbol{v}) - \kappa\, (\boldsymbol{J}, \boldsymbol{B} \times \boldsymbol{v}) = (\boldsymbol{f}, \boldsymbol{v}) \quad \forall\, \boldsymbol{v} \in \boldsymbol{V}(\operatorname{div} 0). \tag{4.12}$$

Proof. Write $r' := r/(r-1)$. For any $\boldsymbol{v} \in \boldsymbol{L}^{r'}(0,T;\boldsymbol{V}(\operatorname{div} 0))$, from (4.6a) we have

$$\int_0^T [(\partial_t \boldsymbol{u}_\tau, \boldsymbol{v}) + \mathcal{O}(\boldsymbol{u}_\tau^*; \bar{\boldsymbol{u}}_\tau, \boldsymbol{v}) + \mathcal{A}(\bar{\boldsymbol{u}}_\tau, \boldsymbol{v}) - \kappa\, (\boldsymbol{J}_\tau, \boldsymbol{B}_\tau^* \times \boldsymbol{v})] = \int_0^T (\boldsymbol{f}_\tau, \boldsymbol{v}). \tag{4.13}$$

Since $\operatorname{div} \boldsymbol{u}_\tau^* = 0$, we have

$$\begin{aligned}
\int_0^T |\mathcal{O}(\boldsymbol{u}_\tau^*; \bar{\boldsymbol{u}}_\tau, \boldsymbol{v})| &= \int_0^T |\mathcal{O}(\boldsymbol{u}_\tau^*; \boldsymbol{v}, \bar{\boldsymbol{u}}_\tau)| \le \int_0^T \|\boldsymbol{u}_\tau^*\|_{\boldsymbol{L}^4(\Omega)} \|\bar{\boldsymbol{u}}_\tau\|_{\boldsymbol{L}^4(\Omega)} \|\boldsymbol{v}\|_{\boldsymbol{H}^1(\Omega)} \\
&\le C \int_0^T \|\boldsymbol{u}_\tau^*\|_{\boldsymbol{L}^2(\Omega)}^{1/2} \|\boldsymbol{u}_\tau^*\|_{\boldsymbol{H}^1(\Omega)}^{1/2} \|\bar{\boldsymbol{u}}_\tau\|_{\boldsymbol{L}^2(\Omega)}^{1/2} \|\bar{\boldsymbol{u}}_\tau\|_{\boldsymbol{H}^1(\Omega)}^{1/2} \|\boldsymbol{v}\|_{\boldsymbol{H}^1(\Omega)} \\
&\le C \int_0^T \|\boldsymbol{u}_\tau^*\|_{\boldsymbol{H}^1(\Omega)}^{1/2} \|\bar{\boldsymbol{u}}_\tau\|_{\boldsymbol{H}^1(\Omega)}^{1/2} \|\boldsymbol{v}\|_{\boldsymbol{H}^1(\Omega)} \\
&\le C \|\boldsymbol{v}\|_{\boldsymbol{L}^2(0,T;\boldsymbol{H}^1(\Omega))}.
\end{aligned}$$

The diffusion term satisfies

$$\int_0^T |\mathcal{A}(\bar{\boldsymbol{u}}_\tau, \boldsymbol{v})| \le C \|\bar{\boldsymbol{u}}_\tau\|_{\boldsymbol{L}^2(0,T;\boldsymbol{H}^1(\Omega))} \|\boldsymbol{v}\|_{\boldsymbol{L}^2(0,T;\boldsymbol{H}^1(\Omega))} \le C \|\boldsymbol{v}\|_{\boldsymbol{L}^2(0,T;\boldsymbol{H}^1(\Omega))}.$$

By arguments similar to (4.10), the Lorenz force term satisfies

$$\begin{aligned}
\int_0^T |(\boldsymbol{J}_\tau \times \boldsymbol{B}_\tau^*, \boldsymbol{v})| &\le C \|\boldsymbol{J}_\tau\|_{\boldsymbol{L}^2(0,T;\boldsymbol{L}^2(\Omega))} \|\mathbf{curl}\, \boldsymbol{B}_\tau^*\|_{\boldsymbol{L}^2(0,T;\boldsymbol{L}^2(\Omega))}^{1/r} \|\boldsymbol{v}\|_{\boldsymbol{L}^{r'}(0,T;\boldsymbol{H}^1(\Omega))} \\
&\le C \|\boldsymbol{v}\|_{\boldsymbol{L}^{r'}(0,T;\boldsymbol{H}^1(\Omega))}.
\end{aligned}$$

So $\boldsymbol{J}_\tau \times \boldsymbol{B}_\tau^*$ is τ-uniformly bounded in $\boldsymbol{L}^r(0,T;\boldsymbol{V}(\operatorname{div} 0)')$ and have a weakly convergent subsequence. By Lemma 4.5, we can extract a subsequence of $\boldsymbol{J}_\tau \times \boldsymbol{B}_\tau^*$ which converges weakly to $\boldsymbol{J} \times \boldsymbol{B}$ in $\boldsymbol{L}^1(0,T;\boldsymbol{L}^{6/5}(\Omega))$. This means

$$\boldsymbol{J}_\tau \times \boldsymbol{B}_\tau^* \rightharpoonup \boldsymbol{J} \times \boldsymbol{B} \quad \text{weakly in } \ \boldsymbol{L}^r(0,T;\boldsymbol{V}(\operatorname{div} 0)').$$

Since $\boldsymbol{f}_\tau$ is τ-uniformly bounded in $\boldsymbol{L}^2(0,T;\boldsymbol{L}^2(\Omega))$, we conclude from the above analyses that $\partial_t \boldsymbol{u}_\tau$ is τ-uniformly bounded in $\boldsymbol{L}^r(0,T;\boldsymbol{V}(\operatorname{div} 0)')$. There is a subsequence such that

$$\partial_t \boldsymbol{u}_\tau \rightharpoonup \partial_t \boldsymbol{u} \quad \text{weakly in } \ \boldsymbol{L}^r(0,T;\boldsymbol{V}(\operatorname{div} 0)').$$

Moreover, by Lemma 4.4, we can extract a subsequence of $\boldsymbol{u}_\tau$ which converges strongly to $\boldsymbol{u}$ in $\boldsymbol{L}^2(0,T;\boldsymbol{L}^4(\Omega))$. Passage $k \to \infty$ on both sides of (4.13) shows that, for any $\boldsymbol{v} \in \boldsymbol{L}^{r'}(0,T;\boldsymbol{V}(\operatorname{div} 0))$,

$$\int_0^T [(\partial_t \boldsymbol{u}, \boldsymbol{v}) + \mathcal{O}(\boldsymbol{u};\boldsymbol{u},\boldsymbol{v}) + \mathcal{A}(\boldsymbol{u},\boldsymbol{v}) - \kappa\, (\boldsymbol{J}, \boldsymbol{B} \times \boldsymbol{v})] = \int_0^T (\boldsymbol{f}, \boldsymbol{v}).$$

This yields (4.12). □

Now based on Lemma 4.5 and Lemma 4.6, we are in a position to prove Theorem 4.2.

Proof of Theorem 4.2. From Lemma 4.5, we know that

$$-\partial_t \boldsymbol{A}_\tau = \boldsymbol{J}_\tau + \boldsymbol{B}_\tau^* \times \bar{\boldsymbol{u}}_\tau \rightharpoonup \boldsymbol{J} + \boldsymbol{B} \times \boldsymbol{u} \quad \text{weakly in } \ \boldsymbol{L}^r(0,T;\boldsymbol{L}^2(\Omega)).$$

Suppose $\mathcal{P}(\boldsymbol{B}_\tau^* \times \bar{\boldsymbol{u}}_\tau) = \nabla \phi_\tau$ with $\phi_\tau \in H_0^1(\Omega)$. By (4.9), there is a constant $C > 0$ independent of τ such that

$$\|\nabla \phi_\tau\|_{\boldsymbol{L}^r(0,T;\boldsymbol{L}^2(\Omega))} \le \|\boldsymbol{B}_\tau^* \times \bar{\boldsymbol{u}}_\tau\|_{\boldsymbol{L}^r(0,T;\boldsymbol{L}^2(\Omega))} \le C.$$

Since $\partial_t \boldsymbol{A}_\tau + \boldsymbol{B}_\tau^* \times \bar{\boldsymbol{u}}_\tau = \partial_t \boldsymbol{a}_\tau + \mathcal{Q}(\boldsymbol{B}_\tau^* \times \bar{\boldsymbol{u}}_\tau)$, we have $\partial_t \boldsymbol{A}_\tau = \partial_t \boldsymbol{a}_\tau + \nabla \phi_\tau$ or

$$\boldsymbol{A}_\tau = \boldsymbol{a}_\tau + \nabla \psi_\tau, \qquad \psi_\tau(t) = \int_0^t \phi_\tau(s) \mathrm{d}s.$$

Therefore, $\boldsymbol{A}_\tau$ are uniformly bounded in $\boldsymbol{W}^{1,r}(0,T;\boldsymbol{C})$. There are a subsequence and a $\psi \in W^{1,r}(0,T;H_0^1(\Omega))$ such that

$$\boldsymbol{A}_\tau \rightharpoonup \boldsymbol{A} := \boldsymbol{a} + \nabla \psi \in \boldsymbol{W}^{1,r}(0,T;\boldsymbol{C})$$

This yields $\boldsymbol{J} = -\partial_t \boldsymbol{A} - \boldsymbol{B} \times \boldsymbol{u}$. Finally, Theorem 4.2 is proven by substituting the expressions of $\boldsymbol{J}$ and $\boldsymbol{A}$ into (4.11) and (4.12). $\square$

5. A preconditioner for the discrete problem

The purpose of this section is to propose a preconditioner for to accelerate the iterative solution of (3.5). Instead of seeking $\bar{\mathbf{u}}_n$ in the divergence-free finite element space, we introduce a Lagrangian multiplier P_n and seek $\bar{\mathbf{u}}_n$ in the unconstrained space $\boldsymbol{V}_h$. In fact, P_n is a piecewise constant approximation of the pressure and will belong to the space

$$Q_h := D_0(\mathcal{T}_h)/\mathbb{R}.$$

For any $\boldsymbol{\Psi} = (\boldsymbol{u}, \boldsymbol{\psi})$, $\boldsymbol{\Phi} = (\boldsymbol{v}, \boldsymbol{c})$ with $\boldsymbol{u}, \boldsymbol{v} \in \boldsymbol{V}_h$ and $\boldsymbol{\psi}, \boldsymbol{c} \in \boldsymbol{C}_h$, based on (3.10) define

$$a_1(\boldsymbol{\Psi}, \boldsymbol{\Phi}) = a(\boldsymbol{\Psi}, \boldsymbol{\Phi}) + 2\tau^{-1}(\operatorname{div} \boldsymbol{u}, \operatorname{div} \boldsymbol{v}).$$

The resulting augmented version of (3.5) reads: Find $\bar{\boldsymbol{\Psi}}_n \in \boldsymbol{V}_h \times \boldsymbol{C}_h$ and $\mathrm{P}_n \in Q_h$ such that

$$a_1(\bar{\boldsymbol{\Psi}}_n, \boldsymbol{\Phi}) - (\operatorname{div} \boldsymbol{v}, \mathrm{P}_n) = f(\boldsymbol{\Phi}) \qquad \forall\, \boldsymbol{\Phi} = (\boldsymbol{v}, \boldsymbol{c}) \in \boldsymbol{V}_h \times \boldsymbol{C}_h, \tag{5.1a}$$

$$(\operatorname{div} \bar{\mathbf{u}}_n, q) = 0 \qquad \forall\, q \in Q_h. \tag{5.1b}$$

Since $\operatorname{div} \bar{\mathbf{u}}_n = 0$ from (5.1b), it holds actually

$$a_1(\bar{\boldsymbol{\Psi}}_n, \boldsymbol{\Phi}) = a(\boldsymbol{\Psi}_n, \boldsymbol{\Phi}) \qquad \forall\, \boldsymbol{\Phi} \in \boldsymbol{V}_h(\operatorname{div} 0) \times \boldsymbol{C}_h.$$

This yields the (algebraic) equivalence of (3.9) and (5.1). The term $2\tau^{-1}(\operatorname{div} \bar{\mathbf{u}}_n, \operatorname{div} \boldsymbol{v})$ does not affect the discrete solutions, but enhances the stability of the mixed formulation. Remember that we have already proven the existence and uniqueness of $\bar{\mathbf{u}}_n$, $\bar{\mathbf{A}}_n$. The pressure $\mathrm{P}_n \in Q_h$ is determined by

$$(\operatorname{div} \boldsymbol{v}, \mathrm{P}_n) = a_1(\bar{\boldsymbol{\Psi}}_n, \boldsymbol{\Phi}) - f(\boldsymbol{\Phi}) \qquad \forall\, \boldsymbol{v} \in \boldsymbol{V}_h.$$

Clearly the linear problem (5.1) can be written into an algebraic form

$$\begin{pmatrix} \mathbb{F} & \mathbb{B}^\top & \mathbb{J}^\top \\ \mathbb{B} & 0 & 0 \\ \mathbb{J} & 0 & \mathbb{C} \end{pmatrix} \begin{pmatrix} \boldsymbol{x}_u \\ \boldsymbol{x}_p \\ \boldsymbol{x}_a \end{pmatrix} = \begin{pmatrix} \boldsymbol{B}_u \\ \boldsymbol{B}_p \\ \boldsymbol{B}_a \end{pmatrix}, \tag{5.2}$$

where $\boldsymbol{x}_u, \boldsymbol{x}_p, \boldsymbol{x}_a$ are vectors of DOFs belonging to $\bar{\mathbf{u}}_n$, P_n, $\bar{\mathbf{A}}_n$ respectively and $\boldsymbol{B}_u, \boldsymbol{B}_p, \boldsymbol{B}_a$ are the corresponding load vectors. Let $\mathbb{A}$ denote the stiffness matrix. Its sub-matrices $\mathbb{F}$, $\mathbb{B}$, $\mathbb{J}$, $\mathbb{C}$ are the Galerkin matrices for the fluid terms, the pressure term, the coupling between $\bar{\mathbf{u}}_n$ and $\bar{\mathbf{A}}_n$, and the magnetic potential terms respectively, namely,

$$\mathbb{F} \leftrightarrow a_1((\bar{\mathbf{u}}_n, 0), (\boldsymbol{v}, 0)), \qquad \mathbb{B} \leftrightarrow -(\mathrm{div}\,\boldsymbol{v}, \mathrm{P}_n),$$
$$\mathbb{C} \leftrightarrow a_1((0, \bar{\mathbf{A}}_n), (0, \boldsymbol{c})), \qquad \mathbb{J} \leftrightarrow \frac{2\kappa}{\tau}\left(\boldsymbol{c}, \mathbf{B}_n^* \times \bar{\mathbf{u}}_n\right).$$

Of course, we suppose that the finite element spaces have been equipped with bases of locally supported functions.

To construct a preconditioner for $\mathbb{A}$, we drop $\mathbb{J}$ and get

$$\mathbb{A} \sim \mathbb{A}_0 = \begin{pmatrix} \mathbb{F} & \mathbb{B}^\top & \mathbb{J}^\top \\ \mathbb{B} & 0 & 0 \\ 0 & 0 & \mathbb{C} \end{pmatrix}.$$

It suffices to study the preconditioner for the 2×2 Navier-Stokes block and the preconditioner for the Maxwell block $\mathbb{C}$ respectively.

Note that $\mathbb{C}$ is just the stiffness matrix of the Maxwell equation without advection. It can be preconditioned by the auxiliary space preconditioning method proposed in Ref. [20]. For the Navier-Stokes block of the stiffness matrix, we consider the LU-decomposition

$$\begin{pmatrix} \mathbb{F} & \mathbb{B}^\top \\ \mathbb{B} & 0 \end{pmatrix} = \begin{pmatrix} \mathbb{I} & 0 \\ \mathbb{B}\mathbb{F}^{-1} & \mathbb{I} \end{pmatrix} \begin{pmatrix} \mathbb{F} & \mathbb{B}^\top \\ 0 & -\mathbb{B}\mathbb{F}^{-1}\mathbb{B}^\top \end{pmatrix}.$$

Inspired by Ref. [6], we approximate the Schur complement as follows

$$\mathbb{B}\mathbb{F}^{-1}\mathbb{B}^\top \approx \mathbb{Q}_p, \qquad \mathbb{Q}_p = \frac{\tau}{2}\left(\int_\Omega q_i q_j\right),$$

where $2\tau^{-1}\mathbb{Q}_p$ is the mass matrix on the pressure finite element space and $\{q_i\}$ is the basis of Q_h. Therefore, we can choose the right matrix of the LU-decomposition as a preconditioner of the Navier-Stokes block, namely,

$$\begin{pmatrix} \mathbb{F} & \mathbb{B}^\top \\ \mathbb{B} & 0 \end{pmatrix} \sim \begin{pmatrix} \mathbb{F} & \mathbb{B}^\top \\ 0 & -\mathbb{B}\mathbb{F}^{-1}\mathbb{B}^\top \end{pmatrix} \sim \begin{pmatrix} \mathbb{F} & \mathbb{B}^\top \\ 0 & -\mathbb{Q}_p \end{pmatrix}.$$

To summarize, we propose an iterative solver for (5.2). In each time step, the initial guess for $(\boldsymbol{x}_u, \boldsymbol{x}_p, \boldsymbol{x}_a)$ is chosen as the solution in the previous time step. Given an approximation $(\tilde{\boldsymbol{x}}_u, \tilde{\boldsymbol{x}}_p, \tilde{\boldsymbol{x}}_a)$ of $(\boldsymbol{x}_u, \boldsymbol{x}_p, \boldsymbol{x}_a)$, let $(\boldsymbol{e}_u, \boldsymbol{e}_p, \boldsymbol{e}_a)$ be the corrections for $(\tilde{\boldsymbol{x}}_u, \tilde{\boldsymbol{x}}_p, \tilde{\boldsymbol{x}}_a)$ and let $(\boldsymbol{r}_u, \boldsymbol{r}_p, \boldsymbol{r}_a)$ be the corresponding residual vectors. We present the algorithm for solving the residual equation

$$\begin{pmatrix} \mathbb{F} & \mathbb{B}^\top & \mathbb{J}^\top \\ 0 & -\mathbb{Q}_p & 0 \\ 0 & 0 & \mathbb{C} \end{pmatrix} \begin{pmatrix} \boldsymbol{e}_u \\ \boldsymbol{e}_p \\ \boldsymbol{e}_a \end{pmatrix} = \begin{pmatrix} \boldsymbol{r}_u \\ \boldsymbol{r}_p \\ \boldsymbol{r}_a \end{pmatrix}. \tag{5.3}$$

The total computational cost for solving (5.2) is insensitive to the tolerance $10^{-4} \leq \varepsilon_0 \leq 10^{-1}$ for solving (5.3). For convenience, we set the tolerance by 10^{-3} for all inner iterations in Algorithm 5.1.

Algorithm 5.1. The residual equation is solved approximately in three steps:

(1) Solve $\mathbb{C}\boldsymbol{e}_a = \boldsymbol{r}_a$ by the CG method with the auxliary space preconditioner from Ref. [20] such that the relative residual is reduced to be less than 10^{-3}.
(2) Solve $\mathbb{Q}_p\boldsymbol{e}_p = -\boldsymbol{r}_p$ by the CG method with diagonal preconditioner such that the relative residual is reduced to be less than 10^{-3}.
(3) Solve $\mathbb{F}\boldsymbol{e}_u = \boldsymbol{r}_u - \mathbb{B}^\top\boldsymbol{e}_p - \mathbb{J}^\top\boldsymbol{e}_a$ by the GMRES method with the additive Schwarz preconditioner (cf. Ref. [8]) such that the relative residual is reduced to be less than 10^{-3}.

6. Numerical experiments

In this section, we confirm the prediction of the theory and demonstrate the robustness of the solver by five numerical experiments. Our implementation is based on the adaptive finite element package "Parallel Hierarchical Grid" (PHG) (cf. Ref. [39]) and the computations are carried out on the cluster LSSC-III of the State Key Laboratory on Scientific and Engineering Computing, Chinese Academy of Sciences.

The first example is to show the efficiency of the solver for the linearly extrapolated scheme (3.5) compared with the nonlinear solver for the Crank-Nicolson scheme (3.3). The second example is to show the convergence rate of the fully discrete scheme. The third example is to demonstrate the optimality of the preconditioner with respect to the number of DOFs and the robustness of the preconditioner for relatively large parameters. The fourth example is the benchmark problem for a three-dimensional driven cavity flow. With this example, we validate the $\boldsymbol{A}$-based MHD formulation (2.6) and demonstrate the robustness of the preconditioner. In both examples, we set the penalty parameter to $\alpha = 10$ and use the computational domain $\Omega = (0,1)^3$. The last example compares the magnitude of the artificial dissipation, which is introduced by the upwind flux, with the magnitudes of viscous dissipation and the Ohmic heating.

Example 6.1. This example is to confirm the efficiency of the linearly extrapolated scheme (3.5) compared with the nonlinear Crank-Nicolson scheme (3.3). The physical parameters are given by $R_e = R_m = \kappa = 1$ and the terminal time $T = 1$. The right-hand sides and the Dirichlet boundary conditions are chosen so that the true solutions are given by

$$\boldsymbol{u} = \left(ye^{-t}, z\cos t, x\right), \quad p = 0, \quad \boldsymbol{A} = (z, 0, y\cos t)\,.$$

Note that the exact solutions are linear in space. The discretization error is mainly due to discretization in time. We fix a tetrahedral mesh with $h = 0.433$ and test the convergence rate with respect to the timestep. In each time step, if we choose the initial guess by $\bar{\mathbf{u}}_n = \mathbf{u}_{n-1}$ and $\bar{\mathbf{A}}_n = \mathbf{A}_{n-1}$ and use *only one* nonlinear iteration, the Crank-Nicolson (C-N) scheme (3.3) will yield a first-order approximation to the continuous problem, while the linearly extrapolated scheme (3.5) is second-order. Let the approximation errors at the final time $t = T$ be denoted by

$$\boldsymbol{e}_u = \boldsymbol{u}(T) - \mathbf{u}_N, \quad e_p = p(T) - \mathrm{P}_N, \quad \boldsymbol{e}_a = \boldsymbol{A}(T) - \mathbf{A}_N.$$

We set the tolerance for iteratively solving linear systems of equations to $\varepsilon = 10^{-10}$. Table 1 shows that the convergence rate for the C-N scheme with one Picard iteration is first-order, namely,

$$\|\boldsymbol{e}_u\|_{1,h} \sim \tau, \qquad \|e_p\|_{L^2(\Omega)} \sim \tau, \qquad \|\boldsymbol{e}_a\|_{\boldsymbol{H}(\mathbf{curl},\Omega)} \sim \tau.$$

Table 2 shows that the second-order convergence is obtained for the linearly extrapolated scheme

$$\|\boldsymbol{e}_u\|_{1,h} \sim \tau^2, \qquad \|e_p\|_{L^2(\Omega)} \sim \tau^2, \qquad \|\boldsymbol{e}_a\|_{\boldsymbol{H}(\mathbf{curl},\Omega)} \sim \tau^2.$$

Table 1. Convergence rates for the C-N scheme at $t = T$ with $m = 1$ and $\varepsilon = 10^{-10}$ (Example 6.1).

τ	$\|\boldsymbol{e}_u\|_{1,h}$	order	$\|e_p\|_{L^2}$	order	$\|\boldsymbol{e}_a\|_{\boldsymbol{H}(\mathbf{curl})}$	order	$\|\mathrm{div}\,\mathbf{u}_N\|_{L^2}$
0.200	7.99e-4	–	9.40-3	–	9.62e-3	–	1.51e-8
0.100	3.79e-4	1.08	1.71e-2	-0.86	5.03e-3	0.94	2.84e-9
0.050	1.90e-4	1.00	8.46e-3	1.02	2.56e-3	0.97	1.15e-9
0.025	9.47e-5	1.00	4.21e-3	1.00	1.29e-3	0.99	1.47e-10

Table 2. Convergence rates for the linearly extrapolated scheme at $t = T$. (Example 6.1).

τ	$\|\boldsymbol{e}_u\|_{1,h}$	order	$\|e_p\|_{L^2}$	order	$\|\boldsymbol{e}_a\|_{\boldsymbol{H}(\mathbf{curl})}$	order	$\|\mathrm{div}\,\mathbf{u}_N\|_{L^2}$
0.200	1.74e-4	–	2.71e-3	–	1.5e-3	–	1.53e-8
0.100	2.40e-5	2.86	1.09e-3	1.31	3.97e-4	1.92	3.79e-9
0.050	5.14e-6	2.22	2.70e-4	2.01	1.02e-4	1.96	1.83e-9
0.025	1.29e-6	1.99	6.69e-5	2.01	2.58e-5	1.98	2.74e-10

In fact, second-order convergence can be obtained for the C-N scheme by multiple Picard iterations, but with higher computational cost. To save computing time, we set the tolerance for solving linear systems of equations to $\varepsilon = 10^{-5}$. Table 3–5 show the convergence rates for the C-N schemes with $m = 2, 3, 4$ iterations respectively. Clearly we also get the second-order convergence for $m = 3, 4$.

To test the relative efficiency of the linear scheme to the nonlinear scheme, we compare both the errors and the computing time for $T = 10$. We choose $\tau = 1/80$, $\varepsilon = 10^{-10}$ for the linearly extrapolated scheme and $\tau = 1/40$, $\varepsilon = 10^{-5}$ for the

Table 3. Convergence rates for the C-N scheme at the final time with $m = 2$ (Example 6.1).

τ	$\Vert \boldsymbol{e}_u \Vert_{1,h}$	order	$\Vert e_p \Vert_{L^2}$	order	$\Vert \boldsymbol{e}_a \Vert_{\boldsymbol{H}(\mathbf{curl})}$	order	$\Vert \mathrm{div}\, \mathbf{u}_N \Vert_{L^2}$
0.200	1.47e-4	–	8.60-4	–	8.20e-4	–	4.60e-7
0.100	5.54e-5	1.41	4.81e-4	0.84	2.79e-4	1.56	2.69e-7
0.050	1.86e-5	1.57	1.31e-4	1.88	9.25e-5	1.59	2.15e-8
0.025	5.71e-6	1.70	3.51e-5	1.90	3.02e-5	1.61	2.93e-9

Table 4. Convergence rates for the C-N scheme at the final time with $m = 3$ (Example 6.1).

τ	$\Vert \boldsymbol{e}_u \Vert_{1,h}$	order	$\Vert e_p \Vert_{L^2}$	order	$\Vert \boldsymbol{e}_a \Vert_{\boldsymbol{H}(\mathbf{curl})}$	order	$\Vert \mathrm{div}\, \mathbf{u}_N \Vert_{L^2}$
0.200	7.63e-5	–	7.36e-4	–	7.49e-4	–	1.87e-8
0.100	1.78e-5	2.10	4.43e-4	0.78	2.07e-4	1.86	8.22e-9
0.050	4.44e-6	2.00	1.12e-4	1.98	5.33e-5	1.96	5.47e-10
0.025	1.13e-6	1.97	2.80e-5	2.00	1.35e-5	1.98	3.85e-11

Table 5. Convergence rates for the C-N scheme at the final time with $m = 4$ (Example 6.1).

τ	$\Vert \boldsymbol{e}_u \Vert_{1,h}$	order	$\Vert e_p \Vert_{L^2}$	order	$\Vert \boldsymbol{e}_a \Vert_{\boldsymbol{H}(\mathbf{curl})}$	order	$\Vert \mathrm{div}\, \mathbf{u}_N \Vert_{L^2}$
0.200	7.60e-5	–	7.29e-4	–	7.44e-4	–	9.60e-10
0.100	1.77e-5	2.10	4.40e-4	0.73	2.05e-4	1.86	3.35e-10
0.050	4.40e-6	2.01	1.11e-4	1.99	5.29e-5	1.95	1.26e-11
0.025	1.11e-6	1.99	2.79e-5	1.99	1.34e-5	1.98	1.22e-11

Crank-Nicolson scheme. We use $m = 2, 3$ Picard iterations for the nonlinear solver respectively. Table 6 shows that the linearly extrapolated scheme is more efficient for long-time simulations.

Table 6. The extrapolated scheme and the C-N scheme with m Picard iterations ($T = 10$).

Schemes	τ	Time (s)	$\vert \boldsymbol{e}_u \vert_{1,h}$	$\Vert e_p \Vert_{L^2(\Omega)}$	$\Vert \boldsymbol{e}_a \Vert_{\boldsymbol{H}(\mathbf{curl},\Omega)}$
linear	1/80	2842	1.05e-6	1.92e-5	3.41e-5
C-N ($m = 2$)	1/40	2877	3.78e-6	6.44e-4	9.92e-5
C-N ($m = 3$)	1/40	4266	1.46e-6	2.62e-5	9.36e-5

Example 6.2. This example is to test the convergence rate for the linearly extrapolated scheme where both the timestep and the meshwidth are refined simultaneously. The physical parameters are given by $R_e = R_m = \kappa = 1$ and the terminal time $T = 0.2$. The right-hand sides and the Dirichlet boundary conditions are chosen so

that the true solutions are given by

$$\boldsymbol{u} = (\sin t \sin y, 0, 0), \quad p = x + y + z - 1.5, \quad \boldsymbol{A} = (0, \sin(t+x), 0).$$

We set the timestep by $\tau_0 = 0.05$ and the meshwidth by $h_0 = 0.866$ initially and then bisect them successively. Table 7 shows the errors at the final time T. Asymptotically, we find that

$$\begin{aligned}
&\|\boldsymbol{e}_u\|_{\boldsymbol{L}^2(\Omega)} \sim O(\tau^2 + h^2),\ \|\boldsymbol{e}_a\|_{\boldsymbol{L}^2(\Omega)} \sim O(\tau^2 + h^2),\\
&|\boldsymbol{e}_u|_{1,h} \sim O(\tau^2 + h), \qquad \|\boldsymbol{e}_a\|_{\boldsymbol{H}(\mathbf{curl},\Omega)} \sim O(\tau^2 + h),\ \|e_p\|_{L^2(\Omega)} \sim O(\tau^2 + h).
\end{aligned}$$

Table 7. Optimal convergence in $\boldsymbol{L}^2(\Omega)$ norms (Example 6.2).

(τ, h)	$\|\boldsymbol{e}_u\|_{L^2}$	$\|\boldsymbol{e}_u\|_{1,h}$	$\|e_p\|_{L^2}$	$\|\boldsymbol{e}_a\|_{L^2}$	$\|\boldsymbol{e}_a\|_{\boldsymbol{H}(\mathbf{curl})}$
(τ_0, h_0)	7.6e-4	1.3e-2	1.8e-1	1.0e-2	7.5e-2
$(\tau_0, h_0)/2$	1.9e-4	6.2e-3	8.9e-2	2.7e-3	3.7e-2
$(\tau_0, h_0)/4$	4.9e-5	3.0e-3	4.4e-2	6.9e-4	1.8e-2
$(\tau_0, h_0)/8$	1.3e-5	1.5e-3	2.2e-2	1.7e-4	9.1e-3

Example 6.3. This example is to test the optimality of the preconditioner given by Algorithm 5.1 with respect to the number of DOFs. We also show the robustness of the preconditioner for relatively large physical parameters and for large timestep. Here we set $R_e = R_m = 100$, $\kappa = 10$ and choose $\tau = 0.1$, $T = 1$.

The initial conditions and the right-hand side are given respectively by

$$\boldsymbol{u}_0 = \left(2y - 2yx^2, 2x - 2xy^2, 0\right), \qquad \boldsymbol{A}_0 = (y, 0, 0), \qquad \boldsymbol{f} = 0.$$

This gives the initial magnetic field $\boldsymbol{B}_0 = (0, 0, 1)$. The boundary conditions are

$$\boldsymbol{u} = \boldsymbol{u}_0, \quad \boldsymbol{A} \times \boldsymbol{n} = \boldsymbol{A}_0 \times \boldsymbol{n} \quad \text{on } \Omega.$$

Table 8 shows the number of GMRES iterations, N_{it}, to reduce the residual of the algebraic system by a factor $\varepsilon = 10^{-10}$. Clearly N_{it} is uniform with respect to h.

Table 8. Optimality of the preconditioned GMRES algorithm (Example 6.3).

h	N_{it}	DOFs for $\mathbf{u}_n$	DOFs for P_n	DOFs for $\mathbf{A}_n$
0.866	12	3.6e+2	4.8e+1	2.0e+2
0.433	12	2.6e+3	3.8e+2	1.2e+3
0.216	12	2.0e+4	3.1e+3	8.4e+3
0.108	12	1.5e+5	2.5e+4	6.2e+4

Example 6.4 (Driven Cavity Flow). This example computes the benchmark problem of driven cavity flow. The right-hand side of the momentum equation is

set to $\boldsymbol{f} = 0$. The initial values are given by $\boldsymbol{A}_0 = (0, 0, y)$, $\boldsymbol{u}_0 = (v, 0, 0)$ where $v \in C^1(\bar{\Omega})$ and satisfies

$$v(x, y, 1) = 1 \qquad \text{and} \qquad v(x, y, z) = 0 \quad \forall\, z \in [0, 1-h].$$

The boundary conditions are set by

$$\boldsymbol{u} = \boldsymbol{u}_0, \quad \boldsymbol{A} \times \boldsymbol{n} = \boldsymbol{A}_0 \times \boldsymbol{n} \qquad \text{on } \partial\Omega.$$

The physical parameters are $R_e = 100, R_m = 200$ and $\kappa = 10$.

For this benchmark problem, we want to compare our results with those in Ref. [23] and to see how the fluid flows under the influence of the magnetic field. Since $\mathbf{A}_n \in \boldsymbol{C}_h$ is piecewise linear, the magnetic induction $\mathbf{B}_n = \mathbf{curl}\,\mathbf{A}_n$ is only piecewise constant. To get a piecewise linear approximation to the magnetic induction, we use Nédélec's second-order edge elements of the second family to compute $\mathbf{A}_n$, see Ref. [27]. Moreover, to capture the boundary layer near the top and the bottom of the cavity, we refine the mesh locally there. The numbers of DOFs are $272, 904$ for $\mathbf{u}_n$, $44, 032$ for P_n, and $440, 781$ for $\mathbf{A}_n$. The timestep is $\tau = 0.01$. The terminal time T is so chosen that the physical fields reach steady state, namely,

$$\frac{\|\mathbf{u}_n - \mathbf{u}_{n-1}\|_{\boldsymbol{L}^2(\Omega)}}{\|\mathbf{u}_n\|_{\boldsymbol{L}^2(\Omega)}} + \frac{\|\mathbf{A}_n - \mathbf{A}_{n-1}\|_{\boldsymbol{L}^2(\Omega)}}{\|\mathbf{A}_n\|_{\boldsymbol{L}^2(\Omega)}} + \frac{\|\mathrm{P}_n - \mathrm{P}_{n-1}\|_{L^2(\Omega)}}{\|\mathrm{P}_n\|_{L^2(\Omega)}} < 10^{-8}.$$

The tolerance for the relative residual of the GMRES method is set to $\varepsilon = 10^{-10}$. Fig 1 shows the convergence history of the preconditioned GMRES method which takes only 10 iterations to reduce the relative residual below ε at $t = 3.98$.

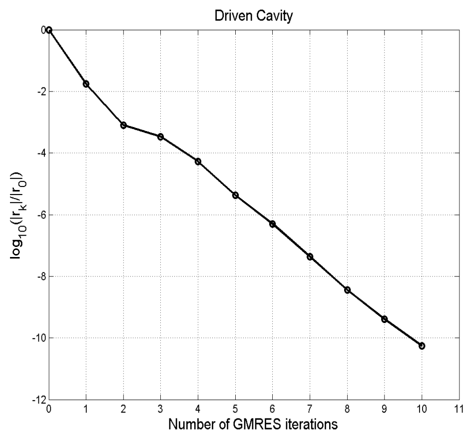

Fig. 1. Convergence history of the preconditioned GMRES method (decay of the relative residual).

The left figure of Fig 2 shows the streamlines of fluid projected onto the cross section $y = 0.5$ and the right one shows the 2D simulation in Ref. [23] where Maxwell's equations are replaced with Poisson's equation for the electric potential.

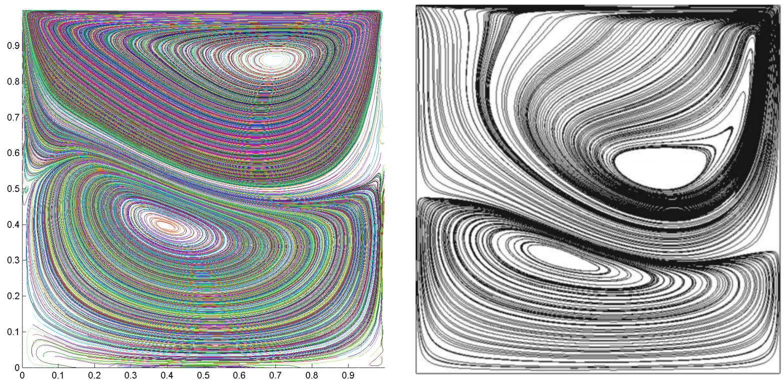

Fig. 2. Projection of the streamlines on the cross section $y = 0.5$. Left: 3D computations by the divergence-free finite element method. Right: 2D computations from [23].

Our 3D results show clearly the flow of the fluid from the upper vortex to the lower vortex. Figure 3 shows the variation of the fluid kinetic energy $\mathsf{E}_{\rm kin}$, the magnetic field energy $\mathsf{E}_{\rm mag}$, and total energy $\mathsf{E} = \mathsf{E}_{\rm kin} + \mathsf{E}_{\rm mag}$ with respect to time, where

$$\mathsf{E}_{\rm kin} = \frac{1}{2} \|\mathbf{u}_n\|^2_{\boldsymbol{L}^2(\Omega)}, \qquad \mathsf{E}_{\rm mag} = \frac{\kappa}{2R_m} \|\mathbf{curl}\,\mathbf{A}_n\|^2_{\boldsymbol{L}^2(\Omega)}.$$

When the fluid tends to the steady state, the total energy and the two portions of the total energy become invariant in time.

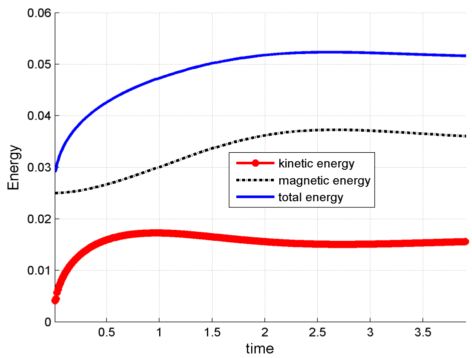

Fig. 3. Variance of fluid kinetic energy, magnetic field energy, and total energy in time.

Figure 4 shows the distribution of the kinetic pressure on three cross sections $x = 0.5$, $y = 0.5$, and $z = 0.5$ respectively. In the middle figure, since the flow is driven from left to right, it generates high pressure regions near the right upper corner. Figure 5 shows magnetic lines of $\boldsymbol{B}_n$ on the cross section $x = 0.5$ and the cross section $y = 0.5$ respectively. Figure 6 shows the eddy current density $\boldsymbol{J}_n$ on the cross section $x = 0.5$ and the cross section $z = 0.5$ respectively. They tells us how the fluid influences the electromagnetic fields.

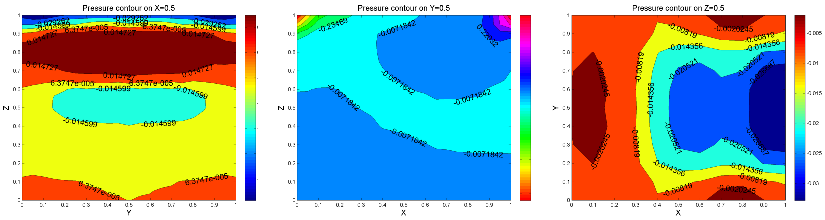

Fig. 4. Pressure contours on three cross sections $x = 0.5$, $y = 0.5$, and $z = 0.5$.

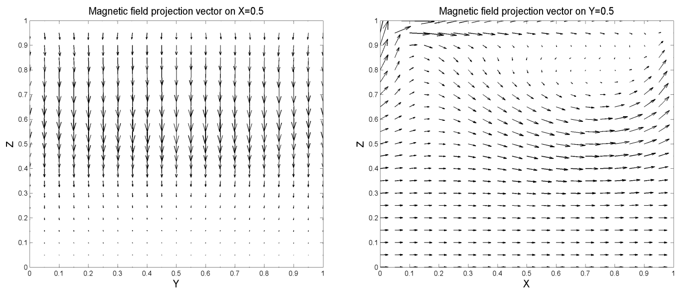

Fig. 5. Projection of $\mathbf{B}_n$ onto two cross sections $x = 0.5$ (left) and $y = 0.5$ (right).

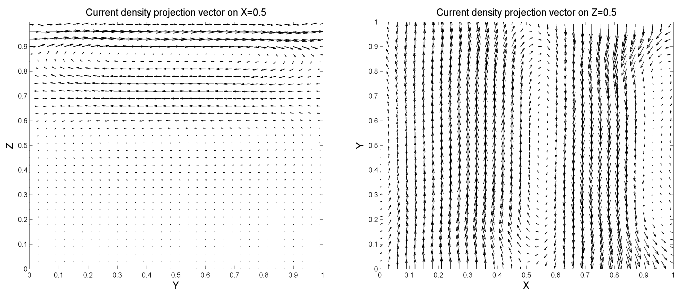

Fig. 6. Projection of $\mathbf{J}_n$ onto two cross sections $x = 0.5$ (left) and $z = 0.5$ (right).

Example 6.5 (Dissipation of the upwind flux). This example compares the magnitude of the artificial dissipation $\mathcal{O}_h(\mathbf{u}_n^*; \bar{\mathbf{u}}_n, \bar{\mathbf{u}}_n)$, which is introduced by the upwind flux, with the magnitudes of other dissipations and the source term in (3.6). The external force and the initial conditions are set by

$$\boldsymbol{f} = (1, \sin x, \sin t), \qquad \boldsymbol{u}_0 = (0, 0, 0), \qquad \boldsymbol{A}_0 = (0, 0, y).$$

The boundary conditions are set by

$$\boldsymbol{u} = 0, \quad \boldsymbol{A} \times \boldsymbol{n} = \boldsymbol{A}_0 \times \boldsymbol{n} \qquad \text{on } \partial\Omega.$$

In this example, we set the physical parameters by $R_e = 100$, $R_m = 10$, $\kappa = 1$ and set the timestep by $\tau = 0.05$. From Table 9, it is clear that the artificial dissipation $\mathcal{O}_h(\mathbf{u}_n^*; \bar{\mathbf{u}}_n, \bar{\mathbf{u}}_n)$ of the upwind flux is negligible compared with the viscous dissipation $\|\bar{\mathbf{u}}_n\|_{\mathcal{A}}^2$, the Ohmic heating $\kappa \|\mathbf{J}_n\|_{\boldsymbol{L}^2(\Omega)}^2$, and the energy supply $(\boldsymbol{f}, \bar{\mathbf{u}}_n)$.

Table 9. Dissipation terms and the source term at $t = 1.0$ (Example 6.5).

h	$\mathcal{O}_h(\mathbf{u}_n^*; \bar{\mathbf{u}}_n, \bar{\mathbf{u}}_n)$	$\|\bar{\mathbf{u}}_n\|_{\mathcal{A}}^2$	$\kappa \|\mathbf{J}_n\|_{\boldsymbol{L}^2(\Omega)}^2$	$\lvert(\boldsymbol{f}, \bar{\mathbf{u}}_n)\rvert$
0.433	2.99e-05	5.97e-03	1.98e-03	1.04e-02
0.217	4.62e-06	5.23e-03	1.91e-03	9.82e-03
0.108	5.44e-07	5.10e-03	1.96e-03	9.86e-03

Acknowledgment

The authors thank the anonymous referee very much for the valuable suggestions and comments. This work is supported in part by the National Center for Mathematics and Interdisciplinary Sciences of China, the State Key Laboratory of Scientific and Engineering Computing of China, and National Magnetic Confinement Fusion Science Program of China (2015GB110003). S. Mao is supported by the National Key Research and Development Program of China (2016YFB0201304), China NSF 11471329, and Youth Innovation Promotion Association of CAS (2016003). W. Zheng is supported in part by the National Science Fund for Distinguished Young Scholars 11725106 and China NSF under the grant 91430215.

References

1. M.A. Abdou et al., On the exploration of innovative concepts for fusion chamber technology, *Fusion Eng. Des.* **54** (2001), 181-247.
2. M.A. Abdou et al., US Plans and strategy for ITER blanket testing, *Fusion Sci. Tech.* **47** (2005), 475-487.
3. F. Armero and J.C. Simo, Long-term dissipativity of time-stepping algorithms for an abstract evolution equation with applications to the incompressible MHD and Navier-Stokes equations, *Comput. Methods Appl. Mech. Engrg.* **131** (1996), 41-90.
4. D.N. Arnold, An interior penalty finite element method with discontinuous elements, *SIAM J. Numer. Anal.* **19** (1982), 742–760.
5. R. Beck, R. Hiptmar, R.H.W. Hoppe, and B. Wohlmoth, Residual based a posteriori error estimations for eddy current computation, *M2AN: Math. Model. Numer. Anal.* **34** (2000), 159C182.
6. M. Benzi and M.A. Olshanskii, Field-of values convergence analysis of augmented Lagrangian preconditioners for the linearized Navier-Stokes problem, *SIAM J. Numer. Anal.* **49** (2011), 770-788.

7. S. Brenner, Poincaré-Friedrichs inequalities for piecewise H^1 functions, *SIAM J. Numer. Anal.* **41** (2003), 306-324.
8. X. Cai and M. Sarkis, A restricted additive Schwarz preconditioner for general sparse linear systems, *SIAM J. Sci. Comput.* **21** (1999), 792–797.
9. B. Cockburn, G. Kanschat, and D. Schötzau, A locally conservative LDG method for the incompressible Navier-Stokes equations, *Math. Comp.* **74** (2004), 1067-1095.
10. J.F. Gerbeau, A stabilized finite element method for the incompressible magnetohydrodynamic equations, *Numer. Math.* **87** (2000), 83–111.
11. J.F. Gerbeau, C. Le Bris, and T. Lelièvre, *Mathematical Methods for the Magnetohydrodynamics of Liquid Metals* (Oxford University Press, 2006).
12. V. Girault and P.-A. Raviart, *Finite element methods for Navier-Stokes Equations* (Springer-Verlag, 1986).
13. V. Girault, B. Riviére, and M.F. Wheeler, A discontinuous Galerkin method with nonoverlapping domain decomposition for the stokes and Navier-Stokes problems, *Math. Comp.* **74** (2004), 53–84.
14. C. Greif, D. Li, D. Schötzau, and X. Wei, A mixed finite element method with exactly divergence-free velocities for incompressible magnetohydrodynamics, *Comput. Methods Appl. Mech. Engrg.* **199** (2010), 2840-2855.
15. J.L. Guermond and P. Minev, Mixed finite element approximation of an MHD problem involving conducting and insulating regions: the 3D case, *Numer. Meth. Part. Diff. Eqns.* **19** (2003), 709–731.
16. M.D. Gunzburger, A.J. Meir, and J.S. Peterson, On the existence and uniqueness and finite element approximation of solutions of the equations of stationary incompressible magnetohydrodynamics, *Math. Comp.* **56** (1991), 523–563.
17. P. Hansbo and M.G. Larson, Discontinuous Galerkin methods for incompressible and nearly incompressible elasticity by Nitsche's method, *Comput. Methods Appl. Mech. Engrg.* **191** (2002), 1895–1908.
18. Y. He, Unconditional convergence of the Euler semi-implicit scheme for the three-dimensional incompressible MHD equations, *IMA J. Numer. Anal.* **35** (2015), 767–801.
19. R. Hiptmair, Finite elements in computational electromagnetism, *Acta Numerica* **11** (2002), 237–339.
20. R. Hiptmair and J. Xu, Nodal auxiliary space preconditioning in $\boldsymbol{H}(\mathbf{curl})$ and $\boldsymbol{H}(\mathrm{div})$ spaces, *SIAM J. Numer. Anal.* **45** (2007), 2483–2509.
21. K. Hu, Y. Ma, and J. Xu, Stable finite element methods preserving $\nabla \cdot \boldsymbol{B} = 0$ exactly for MHD models, *Numer. Math.* **135** (2017), 371–396.
22. Y. Ma, K. Hu, X. Hu, and J. Xu, Robust preconditioners for incompressible MHD models, *J. Comput. Phys.* **316** (2016), 721–746.
23. L. Marioni, F. Bay, and E. Hachem, Numerical stability analysis and flow simulation of lid-driven cavity subjected to high magnetic field, *Phys. Fluids* **28** (2016), 057102.
24. K.A. Mardal and R. Winther, Preconditioning discretizations of systmes of partial differential equations, *Numer Linear Algebra Appl.* **18** (2011), 1–40.
25. P. Monk, *Finite Element Methods for Maxwells Equations* (Oxford University Press, 2003).
26. R. Moreau, *Magnetohydrodynamics* (Kluwer Academic Publishers, 1990).
27. J.C. Nédélec, A new family of mixed finite elements in $\mathbb{R}^3$, *Numer. Math.* **50** (1986), 57–81.
28. M.-J. Ni, R. Munipalli, P. Huang, N.B. Morley, M.A. Abdou, A current density conservative scheme for incompressible MHD flows at a low magnetic Reynolds number. Part I. On a rectangular collocated grid system, *J. Comp. Phys.* **227** (2007), 174–204.

29. M.-J. Ni, R. Munipalli, P. Huang, N.B. Morley, M.A. Abdou, A current density conservative scheme for incompressible MHD flows at a low magnetic Reynolds number. Part II: On an arbitrary collocated mesh, *J. Comp. Phys.* **227** (2007), 205–228.
30. A. Prohl, Convergent finite element discretizations of the nonstationary incompressible magnetohydrodynamics system, *ESAIM: M2AN* **42** (2008), 1065C1087.
31. D. Schötzau, Mixed finite element methods for stationary incompressible magnetohydrodynamics, *Numer. Math.* **96** (2004), 771–800.
32. L.R. Scott and S. Zhang, Finite element interpolation of nonsmooth functions satisfying boundary conditions, *Math. Comp.* **54** (1994), 483-493.
33. R. Temam, *Navier-Stokes Equations, Theory and Numerical Analysis* (North-Holland, 1979).
34. J. Xin, W. Cai, and N. Guo, On the construction of well-conditioned hierarchical bases for $\boldsymbol{H}(\mathrm{div})$-conforming $\mathbb{R}^n$ simplicial elements, *Commun. Comput. Phys.* **14** (2013), 621–638.
35. S. Xu, N. Zhang, and M. Ni, Influence of flow channel insert with pressure equalization opeing on MHD flows in a rectangular duct, *Fusion Eng. Des.* **88** (2013), 271–275.
36. G. Zhang, J. Yang, and C. Bi, Second order unconditionally convergent and energy stable linearized scheme for MHD equations, *Adv. Comput. Math.* (2017), https://doi.org/10.1007/s10444-017-9552-x
37. Y. Zhang, Y. Hou, and L. Shan, Numerical analysis of the Crank-Nicolson extrapolation time discrete scheme for magnetohydrodynamics flows, *Numer. Methods Partial Differential Equations* **31** (2015), 2169–2208.
38. J. Zhang and M. Ni, A consistent and conservative scheme for MHD flows with complex boundaries on an unstructured Cartesian adaptive system, *J. Comp. Phys.* **256** (2014) 520–542.
39. L. Zhang, A parallel algorithm for adaptive local refinement of tetrahedral meshes using bisection, *Numer. Math.: Theor. Method Appl.* **2** (2009), 65–89. (http://lsec.cc.ac.cn/phg)

Appendix A. Discrete compactness

The purpose of this appendix is to prove the compactness and weak compactness for a sequence of DG functions which are uniformly bounded under $\|\cdot\|_{1,h}$.

Lemma A.1. *Let $m > 0$ be an integer and let $\{\xi_k\}_{k=1}^{\infty}$, $\xi_k \in D(m, \mathcal{T}_k)$, be a sequence satisfying*

$$\|\xi_k\|_{1,h} \le C, \qquad n = 1, 2, \cdots,$$

where $C > 0$ is a constant independent of h_k. Then there exist a subsequence of $\{\xi_k\}_{k=1}^{\infty}$ and a $\xi \in H_0^1(\Omega)$ such that

$$\lim_{k\to\infty} \|\xi_k - \xi\|_{L^p(\Omega)} = 0 \qquad \forall\, p \in [1, 6).$$

Proof. It suffices to prove the lemma for $2 \le p < 6$. Let $\tilde{\xi}_k \in L_m(\mathcal{T}_k) \cap H_0^1(\Omega)$ be the Lagrange finite element interpolation of ξ_k defined by, for any $K \in \mathcal{T}_k$,

$$\tilde{\xi}_k(A) = \begin{cases} \xi_k(A), & \text{if } A \text{ is an interior node of } K, \\ \{\!\{\xi_k\}\!\}(A) & \text{if } A \text{ is a node on } \partial K \backslash \Gamma, \\ 0 & \text{if } A \text{ is a node on } \partial K \cap \Gamma. \end{cases} \tag{A.1}$$

By Lemma 3.1, we easily find

$$\left\|\tilde{\xi}_k\right\|_{H^1(\Omega)} \le C \left\|\xi_k\right\|_{1,h} \le C. \tag{A.2}$$

So we can extract a subsequence which converges weakly to some $\xi \in H_0^1(\Omega)$. By the compact injection of $H^1(\Omega)$ into $L^p(\Omega)$ for any $1 \le p < 6$, we can further extract a subsequence, denoted by the same notation, such that

$$\lim_{n\to\infty} \left\|\tilde{\xi}_k - \xi\right\|_{L^p(\Omega)} = 0. \tag{A.3}$$

Let $\mathcal{F}_k$ be the set of all element faces of $\mathcal{T}_k$ and write $\eta_k = \xi_k - \tilde{\xi}_k$. We have

$$\sum_{F\in\mathcal{F}_k} h_F \left\|\eta_k\right\|^2_{L^\infty(F)} \le C \sum_{F\in\mathcal{F}_k} h_F^{-1} \left\|\eta_k\right\|^2_{L^2(F)} \le C \sum_{F\in\mathcal{F}_k} h_F^{-1} \left\|[\![\xi_k]\!]\right\|^2_{L^2(F)} \le C.$$

Using the norm equivalence on $P_k(K)$, we have

$$\begin{aligned}
\left\|\eta_k\right\|^p_{L^p(\Omega)} &\le C \sum_{K\in\mathcal{T}_k} h_K^3 \left\|\eta_k\right\|^p_{L^\infty(\partial K)} \le C \sum_{F\in\mathcal{F}_k} h_F^3 \left\|\eta_k\right\|^p_{L^\infty(F)} \\
&\le C \left(\max_{F\in\mathcal{F}_h} h_F^2 \left\|\eta_k\right\|^{p-2}_{L^\infty(F)}\right) \left(\sum_{F\in\mathcal{F}_k} h_F \left\|\eta_k\right\|^2_{L^\infty(F)}\right) \\
&\le C h_k^{3-p/2} \max_{F\in\mathcal{F}_h} \left(h_F \left\|\eta_k\right\|^2_{L^\infty(F)}\right)^{p/2-1} \le C h_k^{3-p/2}.
\end{aligned}$$

Since $2 \le p < 6$, this shows $\lim_{k\to\infty} \left\|\eta_k\right\|_{L^p(\Omega)} = 0$. We conclude that

$$\lim_{k\to\infty} \left\|\xi_k - \xi\right\|_{L^p(\Omega)} \le \lim_{k\to\infty} \left\|\tilde{\xi}_k - \xi\right\|_{L^p(\Omega)} + \lim_{k\to\infty} \left\|\eta_k\right\|_{L^p(\Omega)} = 0. \qquad \square$$

Lemma A.2. *Let $\{\boldsymbol{\xi}_k\}_{k=1}^\infty \subset \boldsymbol{D}_1(\mathcal{T}_k)$ be uniformly bounded under the norm $\left\|\cdot\right\|_{1,h}$ and let $\{\boldsymbol{\eta}_k\}_{k=1}^\infty \subset \boldsymbol{L}_1(\mathcal{T}_k) \cap \boldsymbol{H}_0^1(\Omega)$ satisfy*

$$\lim_{k\to\infty} \left\|\boldsymbol{\eta}_k - \boldsymbol{\eta}\right\|_{\boldsymbol{H}^1(\Omega)} = 0, \qquad \boldsymbol{\eta} \in \boldsymbol{H}_0^1(\Omega).$$

There exist a subsequence of $\{\boldsymbol{\xi}_k\}_{k=1}^\infty$ and a $\boldsymbol{\xi} \in \boldsymbol{H}_0^1(\Omega)$ such that

$$\lim_{k\to\infty} \mathcal{A}_h(\boldsymbol{\xi}_k, \boldsymbol{\eta}_k) = \mathcal{A}(\boldsymbol{\xi}, \boldsymbol{\eta}). \tag{A.4}$$

Proof. As in the proof of Lemma A.1, let $\tilde{\boldsymbol{\xi}}_k \in \boldsymbol{L}_1(\mathcal{T}_k) \cap \boldsymbol{H}_0^1(\Omega)$ be the Lagrange finite element interpolation of $\boldsymbol{\xi}_k$ defined in (A.1). Since $\boldsymbol{\eta}_k$ is continuous, the formula of integration by part shows that

$$\begin{aligned}
R_e\mathcal{A}_h(\boldsymbol{\xi}_k,\boldsymbol{\eta}_k) &= \sum_{K\in\mathcal{T}_h}\int_K \nabla\boldsymbol{\xi}_k\cdot\nabla\boldsymbol{\eta}_k - \sum_{F\in\mathcal{F}_h}\int_F [\![\boldsymbol{\xi}_k]\!]\left\{\!\!\left\{\frac{\partial\boldsymbol{\eta}_k}{\partial\boldsymbol{n}}\right\}\!\!\right\} \\
&= \sum_{F\in\mathcal{F}_h}\int_F\left(\left[\!\!\left[\boldsymbol{\xi}_k\frac{\partial\boldsymbol{\eta}_k}{\partial\boldsymbol{n}}\right]\!\!\right] - [\![\boldsymbol{\xi}_k]\!]\left\{\!\!\left\{\frac{\partial\boldsymbol{\eta}_k}{\partial\boldsymbol{n}}\right\}\!\!\right\}\right) = \sum_{\substack{F\in\mathcal{F}_h\\ F\cap\Gamma=\emptyset}}\int_F \{\!\{\boldsymbol{\xi}_k\}\!\}\left[\!\!\left[\frac{\partial\boldsymbol{\eta}_k}{\partial\boldsymbol{n}}\right]\!\!\right] \\
&= \sum_{F\in\mathcal{F}_h}\int_F \tilde{\boldsymbol{\xi}}_k\left[\!\!\left[\frac{\partial\boldsymbol{\eta}_k}{\partial\boldsymbol{n}}\right]\!\!\right] = \sum_{K\in\mathcal{T}_h}\int_{\partial K}\tilde{\boldsymbol{\xi}}_k\frac{\partial\boldsymbol{\eta}_k}{\partial\boldsymbol{n}} \\
&= \big(\nabla\tilde{\boldsymbol{\xi}}_k,\nabla\boldsymbol{\eta}_k\big).
\end{aligned}$$

Using (A.2), $\left\{\tilde{\boldsymbol{\xi}}_k\right\}$ is a bounded sequence in $\boldsymbol{H}_0^1(\Omega)$ and thus has a subsequence which converges weakly to some $\boldsymbol{\xi}\in\boldsymbol{H}_0^1(\Omega)$. We deduce that

$$\lim_{k\to\infty} R_e\mathcal{A}_h(\boldsymbol{\xi}_k,\boldsymbol{\eta}_k) = \lim_{k\to\infty}\big(\nabla\tilde{\boldsymbol{\xi}}_k,\nabla\boldsymbol{\eta}\big) = \big(\nabla\boldsymbol{\xi},\nabla\boldsymbol{\eta}\big) = R_e\mathcal{A}(\boldsymbol{\xi},\boldsymbol{\eta}).$$

This completes the proof. □

Appendix B. Proofs of Lemma 4.1 and Lemma 4.2

The purpose of this appendix is to prove Lemma 4.1 and Lemma 4.2. First we prove a useful result for $\boldsymbol{C}_k(\operatorname{div}0)$.

Lemma B.1. *Let* $\{\boldsymbol{g}_k\}_{k=1}^\infty$, $\boldsymbol{g}_k\in\mathcal{Q}_k\boldsymbol{L}^2(\Omega)$, *be a bounded sequence and let* $\boldsymbol{w}_k\in\boldsymbol{C}_k(\operatorname{div}0)$ *be the solution of the discrete electromagnetic problem*

$$(\mathbf{curl}\,\boldsymbol{w}_k,\mathbf{curl}\,\boldsymbol{v}) = (\boldsymbol{g}_k,\boldsymbol{v}) \qquad \forall\,\boldsymbol{v}\in\boldsymbol{C}_k(\operatorname{div}0). \tag{B.1}$$

There exist a subsequence of $\{\boldsymbol{w}_k\}_{k=1}^\infty$ *and a* $\boldsymbol{w}\in\boldsymbol{C}(\operatorname{div}0)$ *such that*

$$\lim_{k\to\infty}\|\boldsymbol{w}_k-\boldsymbol{w}\|_{\boldsymbol{H}(\mathbf{curl},\Omega)} = 0.$$

Proof. By the discrete Poincaré-Friedrichs inequality in (4.3), there is a constant $C>0$ depending only on Ω and the shape-regularity of meshes such that

$$\|\boldsymbol{v}\|_{\boldsymbol{H}(\mathbf{curl},\Omega)} \le C\,\|\mathbf{curl}\,\boldsymbol{v}\|_{\boldsymbol{L}^2(\Omega)} \qquad \forall\,\boldsymbol{v}\in\boldsymbol{C}_k(\operatorname{div}0).$$

Therefore, problem (B.1) has a unique solution and

$$\|\boldsymbol{w}_k\|_{\boldsymbol{H}(\mathbf{curl},\Omega)} \le C\,\|\boldsymbol{g}_k\|_{\boldsymbol{L}^2(\Omega)}.$$

So $\{\boldsymbol{w}_k\}_{k=1}^\infty$ are uniformly bounded under $\|\cdot\|_{\boldsymbol{H}(\mathbf{curl},\Omega)}$. By the discrete compactness of $\boldsymbol{C}_k(\operatorname{div}0)$ [25, Theorem 7.18], there exist a subsequence and a $\boldsymbol{w}\in\boldsymbol{C}$ such that

$$\boldsymbol{w}_k\rightharpoonup\boldsymbol{w}\quad\text{in }\boldsymbol{H}(\mathbf{curl},\Omega),\qquad \boldsymbol{w}_k\to\boldsymbol{w}\quad\text{in }\boldsymbol{L}^2(\Omega).$$

Moreover, for any fixed $l>0$,

$$(\boldsymbol{w},\nabla v) = \lim_{k\to\infty}(\boldsymbol{w}_k,\nabla v) = 0 \qquad \forall\,v\in L_2(\mathcal{T}_l)\cap H_0^1(\Omega).$$

The denseness of $L_2(\mathcal{T}_l)\cap H_0^1(\Omega)$ in $H_0^1(\Omega)$ as $l\to\infty$ shows $\boldsymbol{w}\in\boldsymbol{C}(\operatorname{div}0)$. Similarly, $\boldsymbol{g}_k$ has a subsequence which converges weakly to some $\boldsymbol{g}\in\boldsymbol{H}(\operatorname{div}0,\Omega)$. Therefore,

$$(\mathbf{curl}\,\boldsymbol{w},\mathbf{curl}\,\boldsymbol{v})=(\boldsymbol{g},\boldsymbol{v})\qquad\forall\,\boldsymbol{v}\in\boldsymbol{C}(\operatorname{div}0).\tag{B.2}$$

Let $\Pi_k^{\mathrm{GP}}\colon\boldsymbol{C}\to\boldsymbol{C}_k$ be the Galerkin projection operator defined by

$$(\mathbf{curl}\,\Pi_k^{\mathrm{GP}}\boldsymbol{w},\mathbf{curl}\,\boldsymbol{v})+(\Pi_k^{\mathrm{GP}}\boldsymbol{w},\boldsymbol{v})=(\mathbf{curl}\,\boldsymbol{w},\mathbf{curl}\,\boldsymbol{v})+(\boldsymbol{w},\boldsymbol{v})\qquad\forall\,\boldsymbol{v}\in\boldsymbol{C}_k.$$

The denseness of $\boldsymbol{C}_k$ in $\boldsymbol{C}$ as $k\to\infty$ shows that

$$\lim_{k\to\infty}\left\|\Pi_k^{\mathrm{GP}}\boldsymbol{w}-\boldsymbol{w}\right\|_{\boldsymbol{H}(\mathbf{curl},\Omega)}=0.\tag{B.3}$$

Since $(\boldsymbol{g}_k,\nabla v)=0$ for all $v\in L_2(\mathcal{T}_k)\cap H_0^1(\Omega)$, from (B.1), we also have

$$(\mathbf{curl}\,\boldsymbol{w}_k,\mathbf{curl}\,\boldsymbol{v})=(\boldsymbol{g}_k,\boldsymbol{v})\qquad\forall\,\boldsymbol{v}\in\boldsymbol{C}_k.$$

Similarly, from (B.2), we have

$$(\mathbf{curl}\,\boldsymbol{w},\mathbf{curl}\,\boldsymbol{v})=(\boldsymbol{g},\boldsymbol{v})\qquad\forall\,\boldsymbol{v}\in\boldsymbol{C}_k.$$

Write $\boldsymbol{e}_k=\boldsymbol{w}-\boldsymbol{w}_k$, $\boldsymbol{\xi}_k=\Pi_k^{\mathrm{GP}}\boldsymbol{w}-\boldsymbol{w}_k\in\boldsymbol{C}_k$, and $\boldsymbol{\eta}_k=\boldsymbol{w}-\Pi_k^{\mathrm{GP}}\boldsymbol{w}$. By the strong convergence of $\boldsymbol{w}_k$ in $\boldsymbol{L}^2(\Omega)$, we find that

$$\lim_{k\to\infty}\|\boldsymbol{\xi}_k\|_{\boldsymbol{L}^2(\Omega)}\le\lim_{k\to\infty}\|\boldsymbol{e}_k\|_{\boldsymbol{L}^2(\Omega)}+\lim_{k\to\infty}\|\boldsymbol{\eta}_k\|_{\boldsymbol{L}^2(\Omega)}=0.$$

Since $\boldsymbol{g}_k$ and $\mathbf{curl}\,\boldsymbol{e}_k$ are bounded in $\boldsymbol{L}^2(\Omega)$, by (B.3) we have

$$\begin{aligned}\lim_{k\to\infty}\|\mathbf{curl}\,\boldsymbol{e}_k\|^2_{\boldsymbol{L}^2(\Omega)}&=\lim_{k\to\infty}(\mathbf{curl}\,\boldsymbol{e}_k,\mathbf{curl}\,\boldsymbol{\xi}_k)+\lim_{k\to\infty}(\mathbf{curl}\,\boldsymbol{e}_k,\mathbf{curl}\,\boldsymbol{\eta}_k)\\&=\lim_{k\to\infty}(\boldsymbol{g}-\boldsymbol{g}_k,\boldsymbol{\xi}_k)+\lim_{k\to\infty}(\mathbf{curl}\,\boldsymbol{e}_k,\mathbf{curl}\,\boldsymbol{\eta}_k)=0.\end{aligned}$$

This completes the proof. □

Proof of Lemma 4.1. From Corollary 3.1, $\{\mathbf{u}_n^{(k)}\}_{k=1}^{\infty}$ are uniformly bounded under $\|\cdot\|_{1,h}$. Let $\tilde{\mathbf{u}}_n^{(k)}$ be the Lagrange finite element interpolation of $\mathbf{u}_n^{(k)}$ defined as in (A.1). Then using (A.3), $\{\tilde{\mathbf{u}}_n^{(k)}\}_{k=1}^{\infty}$ are also bounded in $\boldsymbol{V}$ and satisfy

$$\lim_{k\to\infty}\left\|\tilde{\mathbf{u}}_n^{(k)}-\mathbf{u}_n^{(k)}\right\|_{\boldsymbol{L}^p(\Omega)}=0\qquad\forall\,2\le p<6.$$

There is a subsequence of $\tilde{\mathbf{u}}_n^{(k)}$ which converges weakly to some $\boldsymbol{u}_n\in\boldsymbol{V}$ and

$$\lim_{k\to\infty}\left\|\mathbf{u}_n^{(k)}-\boldsymbol{u}_n\right\|_{\boldsymbol{L}^p(\Omega)}=\lim_{k\to\infty}\left\|\tilde{\mathbf{u}}_n^{(k)}-\boldsymbol{u}_n\right\|_{\boldsymbol{L}^p(\Omega)}=0\qquad\forall\,2\le p<6.\tag{B.4}$$

Moreover, since $\operatorname{div}\mathbf{u}_n^{(k)}=0$, we have $\operatorname{div}\boldsymbol{u}_n=0$ by seeing that

$$(\boldsymbol{u}_n,\nabla v)=\lim_{k\to\infty}\left(\tilde{\mathbf{u}}_n^{(k)},\nabla v\right)=\lim_{k\to\infty}\left(\mathbf{u}_n^{(k)},\nabla v\right)=0\qquad\forall\,v\in H_0^1(\Omega).$$

From Corollary 3.1 and the Poincaré-Friedrichs inequality in (4.3), $\mathbf{a}_n^{(k)}$ are uniformly bounded in $\boldsymbol{C}$. We can extract a subsequence which converges weakly to some $\boldsymbol{a}_n\in\boldsymbol{C}$. Similarly, we have

$$(\boldsymbol{a}_n,\nabla v_l)=\lim_{k\to\infty}\left(\mathbf{a}_n^{(k)},\nabla v_l\right)=0\qquad\forall\,v\in L_2(\mathcal{T}_l)\cap H_0^1(\Omega),\ \ l\ge1.$$

By the denseness of $L_2(\mathcal{T}_l) \cap H_0^1(\Omega)$ in $H_0^1(\Omega)$ as $l \to \infty$, we easily obtain

$$(\boldsymbol{a}_n, \nabla v) = 0 \qquad \forall\, v \in H_0^1(\Omega). \tag{B.5}$$

This shows $\boldsymbol{a}_n \in \boldsymbol{C}(\mathrm{div}\, 0)$ for any $1 \le n \le N$.

By (3.5b), $(\mathbf{J}_n^{(k)}, \nabla v_h) = 0$ for all $v_h \in L_2(\mathcal{T}_h) \cap H_0^1(\Omega)$. So we have

$$\mathbf{J}_n^{(k)} = \mathcal{Q}_k \mathbf{J}_n^{(k)} = -\delta_t \mathbf{a}_n^{(k)} - \mathcal{Q}_k(\mathbf{B}_n^{*(k)} \times \bar{\mathbf{u}}_n^{(k)}), \quad \delta_t \mathbf{a}_n^{(k)} := (\mathbf{a}_n^{(k)} - \mathbf{a}_{n-1}^{(k)})/\tau.$$

By Corollary 3.1, $\mathbf{J}_n^{(k)} \in \mathcal{Q}_k \boldsymbol{L}^2(\Omega)$ are uniformly bounded in $\boldsymbol{L}^2(\Omega)$. Equation (2.6b) indicates that $\bar{\mathbf{a}}_n^{(k)} := \big(\mathbf{a}_n^{(k)} + \mathbf{a}_{n-1}^{(k)}\big)/2$ satisfies

$$\big(\mathbf{curl}\, \bar{\mathbf{a}}_n^{(k)}, \mathbf{curl}\, \boldsymbol{c}\big) = R_m\big(\mathbf{J}_n^{(k)}, \boldsymbol{c}\big) \qquad \forall\, \boldsymbol{c} \in \boldsymbol{C}_k(\mathrm{div}\, 0). \tag{B.6}$$

By Lemma B.1, there is a subsequence of $\bar{\mathbf{a}}_n^{(k)}$ which converges strongly to $\bar{\boldsymbol{a}}_n$ in $\boldsymbol{C}(\mathrm{div}\, 0)$. Moreover, by the strong convergence of $\mathbf{a}_0^{(k)}$ and the method of induction, $\mathbf{a}_n^{(k)}$ converges strongly to $\boldsymbol{a}_n$ in $\boldsymbol{C}$ for all $1 \le n \le N$.

By the boundedness of $\mathbf{J}_n^{(k)}$, we can extract a subsequence which converges weakly to a $\boldsymbol{J}_n \in \boldsymbol{L}^2(\Omega)$. Arguments similar to (B.5) show $\mathrm{div}\, \boldsymbol{J}_n = 0$. Note that (B.6) also holds for $\boldsymbol{c} \in \boldsymbol{C}_k$. Using $\boldsymbol{C}_l \subset \boldsymbol{C}_k$ for $l \le k$, we get

$$\big(\mathbf{curl}\, \bar{\mathbf{a}}_n^{(k)}, \mathbf{curl}\, \boldsymbol{c}_l\big) = R_m\big(\mathbf{J}_n^{(k)}, \boldsymbol{c}_l\big) \qquad \forall\, \boldsymbol{c}_l \in \boldsymbol{C}_l.$$

Passage to $k \to \infty$ on both sides of the above equality yields

$$(\mathbf{curl}\, \bar{\boldsymbol{a}}_n, \mathbf{curl}\, \boldsymbol{c}_l) = R_m(\boldsymbol{J}_n, \boldsymbol{c}_l) \qquad \forall\, \boldsymbol{c}_l \in \boldsymbol{C}_l. \tag{B.7}$$

The denseness of $\boldsymbol{C}_l$ in $\boldsymbol{C}$ as $l \to \infty$ shows

$$(\mathbf{curl}\, \bar{\boldsymbol{a}}_n, \mathbf{curl}\, \boldsymbol{c}) = R_m(\boldsymbol{J}_n, \boldsymbol{c}) \qquad \forall\, \boldsymbol{c} \in \boldsymbol{C}. \tag{B.8}$$

By (B.8) and the definition of weak derivatives, we have $\mathbf{curl}\, \bar{\boldsymbol{B}}_n = R_m \boldsymbol{J}_n$. Let $s > 1/2$ be the constant in (4.1). It holds that

$$\bar{\boldsymbol{B}}_n \in \boldsymbol{X}_t \hookrightarrow\hookrightarrow \boldsymbol{H}^s(\Omega) \hookrightarrow \boldsymbol{L}^q(\Omega), \qquad q = 6/(3-2s) > 3. \tag{B.9}$$

The same holds for $\boldsymbol{B}_n$ and $\boldsymbol{B}_n^*$. Then

$$\|\boldsymbol{B}_n^* \times \bar{\boldsymbol{u}}_n\|_{\boldsymbol{L}^2(\Omega)} \le \|\boldsymbol{B}_n^*\|_{\boldsymbol{L}^3(\Omega)} \|\bar{\boldsymbol{u}}_n\|_{\boldsymbol{L}^6(\Omega)} \le C \|\boldsymbol{B}_n^*\|_{\boldsymbol{H}(\mathbf{curl},\Omega)} \|\bar{\boldsymbol{u}}_n\|_{\boldsymbol{H}^1(\Omega)}. \tag{B.10}$$

It justifies the operation of $\mathcal{Q}$ on $\boldsymbol{B}_n^* \times \bar{\boldsymbol{u}}_n$. Since $\delta_t \mathbf{a}_n^{(k)}$ converges strongly to $\delta_t \boldsymbol{a}_n$ in $\boldsymbol{C}$ and $\mathbf{J}_n^{(k)}$ converges weakly to $\boldsymbol{J}_n$ in $\boldsymbol{L}^2(\Omega)$, so $\mathcal{Q}_k(\mathbf{B}_n^{*(k)} \times \bar{\mathbf{u}}_n^{(k)})$ converges weakly in $\boldsymbol{L}^2(\Omega)$. It suffices to show that its limit is $\mathcal{Q}(\boldsymbol{B}_n^* \times \bar{\boldsymbol{u}}_n)$.

For any $\boldsymbol{c} \in \boldsymbol{C}$, the denseness of $L_2(\mathcal{T}_k)$ in $H^1(\Omega)$ as $k \to \infty$ yields

$$\lim_{k\to\infty} \|\mathcal{Q}_k \boldsymbol{c} - \mathcal{Q}\boldsymbol{c}\|_{\boldsymbol{L}^2(\Omega)} = \lim_{k\to\infty} \|\mathcal{P}_k \boldsymbol{c} - \mathcal{P}\boldsymbol{c}\|_{\boldsymbol{L}^2(\Omega)} = 0. \tag{B.11}$$

Since $\mathcal{Q}\boldsymbol{c} \in \boldsymbol{X}_n \hookrightarrow\hookrightarrow \boldsymbol{H}^s(\Omega) \hookrightarrow \boldsymbol{L}^q(\Omega)$, the discrete compactness in Lemma A.1 shows that, for $p = 2q/(q-2) < 6$,

$$\lim_{k\to\infty} \left\| \big(\bar{\mathbf{u}}_n^{(k)} - \bar{\boldsymbol{u}}_n\big) \times \mathcal{Q}\boldsymbol{c} \right\|_{\boldsymbol{L}^2(\Omega)} \le \lim_{k\to\infty} \left\| \bar{\mathbf{u}}_n^{(k)} - \bar{\boldsymbol{u}}_n \right\|_{\boldsymbol{L}^p(\Omega)} \|\mathcal{Q}\boldsymbol{c}\|_{\boldsymbol{L}^q(\Omega)} = 0.$$

Moreover, the strong convergence of $\mathbf{B}_n^{*(k)}$ in $\boldsymbol{L}^2(\Omega)$ shows that

$$\begin{aligned}
&\lim_{k\to\infty}\Big(\mathcal{Q}_k\big(\mathbf{B}_n^{*(k)}\times\bar{\mathbf{u}}_n^{(k)}\big),\boldsymbol{c}\Big)=\lim_{k\to\infty}\Big(\mathcal{Q}_k\big(\mathbf{B}_n^{*(k)}\times\bar{\mathbf{u}}_n^{(k)}\big),\mathcal{Q}_k\boldsymbol{c}\Big)\\
&=\lim_{k\to\infty}\Big(\mathcal{Q}_k\big(\mathbf{B}_n^{*(k)}\times\bar{\mathbf{u}}_n^{(k)}\big),\mathcal{Q}\boldsymbol{c}\Big)=\lim_{k\to\infty}\Big(\mathbf{B}_n^{*(k)}\times\bar{\mathbf{u}}_n^{(k)},\mathcal{Q}\boldsymbol{c}\Big)\\
&=(\boldsymbol{B}_n^*,\bar{\boldsymbol{u}}_n\times\mathcal{Q}\boldsymbol{c})=(\mathcal{Q}(\boldsymbol{B}_n^*\times\bar{\boldsymbol{u}}_n),\boldsymbol{c})\qquad\forall\,\boldsymbol{c}\in\boldsymbol{C}.
\end{aligned}$$

Therefore, $\mathcal{Q}_k\big(\mathbf{B}_n^{*(k)}\times\bar{\mathbf{u}}_n^{(k)}\big)$ converges weakly* to $\mathcal{Q}(\boldsymbol{B}_n^*\times\bar{\boldsymbol{u}}_n)$ in $\boldsymbol{C}'$. $\square$

Proof of Lemma 4.2. First we take any $\boldsymbol{w}\in\boldsymbol{C}_0^\infty(\Omega)\cap\boldsymbol{H}(\operatorname{div}0,\Omega)$ and let $\Pi_k^{\mathrm{SZ}}\boldsymbol{w}\in\boldsymbol{L}_1(\mathcal{T}_k)\cap\boldsymbol{V}$ be its Scott-Zhang interpolation. From [32], we have

$$\big\|\boldsymbol{w}-\Pi_k^{\mathrm{SZ}}\boldsymbol{w}\big\|_{\boldsymbol{H}^m(\Omega)}\le Ch_k^{2-m}\,|\boldsymbol{w}|_{\boldsymbol{H}^2(\Omega)}\,,\qquad m=0,1. \tag{B.12}$$

Let $\Pi_k^{\mathrm{div}}\boldsymbol{w}\in\boldsymbol{V}_k$ be Nédélec's face element interpolation of $\boldsymbol{w}$ from the second family. By Theorem 1 of [27], $\Pi_k^{\mathrm{div}}\boldsymbol{w}$ also respects the divergence-free property

$$\operatorname{div}\big(\Pi_k^{\mathrm{div}}\boldsymbol{w}\big)=0\qquad\text{or}\qquad\Pi_k^{\mathrm{div}}\boldsymbol{w}\in\boldsymbol{V}_k(\operatorname{div}0).$$

Moreover, Proposition 1 of [27] gives the error estimates

$$\big\|\boldsymbol{w}-\Pi_k^{\mathrm{div}}\boldsymbol{w}\big\|_{\boldsymbol{H}^m(K)}\le Ch_k^{2-m}\,|\boldsymbol{w}|_{\boldsymbol{H}^2(K)}\quad\forall\,K\in\mathcal{T}_k,\quad m=0,1.$$

By inverse estimate, we deduce that

$$\begin{aligned}
\big\|\boldsymbol{w}-\Pi_k^{\mathrm{div}}\boldsymbol{w}\big\|_{1,h}&\le\big|\Pi_k^{\mathrm{SZ}}\boldsymbol{w}-\boldsymbol{w}\big|_{\boldsymbol{H}^1(\Omega)}+\big\|\Pi_k^{\mathrm{SZ}}\boldsymbol{w}-\Pi_k^{\mathrm{div}}\boldsymbol{w}\big\|_{1,h}\\
&\le Ch_k\,|\boldsymbol{w}|_{\boldsymbol{H}^2(\Omega)}+Ch_k^{-1}\,\big\|\Pi_k^{\mathrm{SZ}}\boldsymbol{w}-\Pi_k^{\mathrm{div}}\boldsymbol{w}\big\|_{\boldsymbol{L}^2(\Omega)}\\
&\le Ch_k\,|\boldsymbol{w}|_{\boldsymbol{H}^2(\Omega)}\,.
\end{aligned} \tag{B.13}$$

Taking $\boldsymbol{v}=\Pi_k^{\mathrm{div}}\boldsymbol{w}$ in (2.6a) shows that

$$\begin{aligned}
\Big(\delta_t\mathbf{u}_n^{(k)},\Pi_k^{\mathrm{div}}\boldsymbol{w}\Big)+\mathcal{O}_h(\mathbf{u}_n^{*(k)};\bar{\mathbf{u}}_n^{(k)},\Pi_k^{\mathrm{div}}\boldsymbol{w})+\mathcal{A}_h(\bar{\mathbf{u}}_n^{(k)},\Pi_k^{\mathrm{div}}\boldsymbol{w})\\
-\kappa\Big(\mathbf{J}_n^{(k)},\mathbf{B}_n^{*(k)}\times\Pi_k^{\mathrm{div}}\boldsymbol{w}\Big)=(\boldsymbol{f}_n,\Pi_k^{\mathrm{div}}\boldsymbol{w}).
\end{aligned} \tag{B.14}$$

We shall consider the limit of each term on both sides of (B.14) as $k\to\infty$. By (B.13) and Lemma 4.1, we have

$$\lim_{k\to\infty}\Big(\delta_t\mathbf{u}_n^{(k)},\Pi_k^{\mathrm{div}}\boldsymbol{w}\Big)=(\delta_t\boldsymbol{u}_n,\boldsymbol{w})\,,\qquad\lim_{k\to\infty}(\boldsymbol{f}_n,\Pi_k^{\mathrm{div}}\boldsymbol{w})=(\boldsymbol{f}_n,\boldsymbol{w}).$$

The convection term can be split into two terms

$$\mathcal{O}_h(\mathbf{u}_n^{*(k)};\bar{\mathbf{u}}_n^{(k)},\Pi_k^{\mathrm{div}}\boldsymbol{w})=\mathcal{O}_h(\mathbf{u}_n^{*(k)};\bar{\mathbf{u}}_n^{(k)},\boldsymbol{w})+\mathcal{O}_h(\mathbf{u}_n^{*(k)};\bar{\mathbf{u}}_n^{(k)},\Pi_k^{\mathrm{div}}\boldsymbol{w}-\boldsymbol{w}).$$

By Lemma 3.3 and Corollary 3.1, the second term on the right-hand side admits

$$\lim_{k\to\infty}\Big|\mathcal{O}_h(\mathbf{u}_n^{*(k)};\bar{\mathbf{u}}_n^{(k)},\Pi_k^{\mathrm{div}}\boldsymbol{w}-\boldsymbol{w})\Big|\le C\tau^{-2}\lim_{k\to\infty}\big\|\Pi_k^{\mathrm{div}}\boldsymbol{w}-\boldsymbol{w}\big\|_{1,h}=0.$$

Since $\mathbf{u}_n^{*(k)} \cdot \boldsymbol{n}$ is continuous across element faces, the convergence of $\mathbf{u}_n^{(k)}$ shows

$$\begin{aligned}
\lim_{k\to\infty} \mathcal{O}_h(\mathbf{u}_n^{*(k)}; \bar{\mathbf{u}}_n^{(k)}, \boldsymbol{w}) &= -\lim_{k\to\infty} \sum_{K\in\mathcal{T}_k} \int_K \bar{\mathbf{u}}_n^{(k)} \cdot \operatorname{div}\left(\mathbf{u}_n^{*(k)} \otimes \boldsymbol{w}\right) \\
&= -\lim_{k\to\infty} \sum_{K\in\mathcal{T}_k} \int_K \bar{\boldsymbol{u}}_n \cdot \operatorname{div}\left(\mathbf{u}_n^{*(k)} \otimes \boldsymbol{w}\right) \\
&= \lim_{k\to\infty} \left(\nabla \bar{\boldsymbol{u}}_n, \mathbf{u}_n^{*(k)} \otimes \boldsymbol{w}\right) = \mathcal{O}(\boldsymbol{u}_n^*; \bar{\boldsymbol{u}}_n, \boldsymbol{w}).
\end{aligned}$$

Similarly, by Lemma A.2, the diffusion term satisfies

$$\begin{aligned}
\lim_{k\to\infty} \mathcal{A}_h(\bar{\mathbf{u}}_n^{(k)}, \Pi_k^{\mathrm{div}} \boldsymbol{w}) &= \lim_{k\to\infty} \mathcal{A}_h(\bar{\mathbf{u}}_n^{(k)}, \Pi_k^{\mathrm{SZ}} \boldsymbol{w}) + \lim_{k\to\infty} \mathcal{A}_h(\bar{\mathbf{u}}_n^{(k)}, \Pi_k^{\mathrm{div}} \boldsymbol{w} - \Pi_k^{\mathrm{SZ}} \boldsymbol{w}) \\
&= \mathcal{A}(\bar{\boldsymbol{u}}_n, \boldsymbol{w}) + \lim_{k\to\infty} \mathcal{A}_h(\bar{\mathbf{u}}_n^{(k)}, \Pi_k^{\mathrm{div}} \boldsymbol{w} - \Pi_k^{\mathrm{SZ}} \boldsymbol{w}).
\end{aligned}$$

By inverse estimate and (B.12)–(B.13), we deduce that

$$\left|\mathcal{A}_h(\bar{\mathbf{u}}_n^{(k)}, \Pi_k^{\mathrm{div}} \boldsymbol{w} - \Pi_k^{\mathrm{SZ}} \boldsymbol{w})\right| \le C/(\tau h_k) \left\|\Pi_k^{\mathrm{div}} \boldsymbol{w} - \Pi_k^{\mathrm{SZ}} \boldsymbol{w}\right\|_{\boldsymbol{L}^2(\Omega)} \le C h_k/\tau \, |\boldsymbol{w}|_{\boldsymbol{H}^2(\Omega)} .$$

Therefore, the diffusion term satisfies

$$\lim_{k\to\infty} \mathcal{A}_h(\bar{\mathbf{u}}_n^{(k)}, \Pi_k^{\mathrm{div}} \boldsymbol{w}) = \mathcal{A}(\bar{\boldsymbol{u}}_n, \boldsymbol{w}).$$

It is left to study the Lorenz force term. By Lemma 4.1, $\mathbf{J}_n^{(k)}$ converges weakly to $\boldsymbol{J}_n$ and $\mathbf{B}_n^{*(k)}$ converges strongly to $\boldsymbol{B}_n^*$ in $\boldsymbol{L}^2(\Omega)$. Let $q = 6/(3-2s) > 3$ be given in (B.9) and $p := 2q/(q-2) < 6$. By inverse estimate, we deduce that

$$\begin{aligned}
\left\|\boldsymbol{w} - \Pi_k^{\mathrm{div}} \boldsymbol{w}\right\|_{\boldsymbol{L}^p(\Omega)} &\le \left\|\Pi_k^{\mathrm{div}} \boldsymbol{w} - \Pi_k^{\mathrm{SZ}} \boldsymbol{w}\right\|_{\boldsymbol{L}^p(\Omega)} + \left\|\Pi_k^{\mathrm{SZ}} \boldsymbol{w} - \boldsymbol{w}\right\|_{\boldsymbol{L}^p(\Omega)} \\
&\le C h_k^{3/p-3/2} \left\|\Pi_k^{\mathrm{div}} \boldsymbol{w} - \Pi_k^{\mathrm{SZ}} \boldsymbol{w}\right\|_{\boldsymbol{L}^2(\Omega)} + \left\|\Pi_k^{\mathrm{SZ}} \boldsymbol{w} - \boldsymbol{w}\right\|_{\boldsymbol{H}^1(\Omega)} \\
&\le C h_k \, |\boldsymbol{w}|_{\boldsymbol{H}^2(\Omega)} .
\end{aligned}$$

Since $\boldsymbol{B}_n^* \in \boldsymbol{X}_t \hookrightarrow \boldsymbol{L}^q(\Omega)$, this shows

$$\lim_{k\to\infty} \left\|\boldsymbol{B}_n^* \times (\Pi_k^{\mathrm{div}} \boldsymbol{w} - \boldsymbol{w})\right\|_{\boldsymbol{L}^2(\Omega)} \le C \left\|\boldsymbol{B}_n^*\right\|_{\boldsymbol{L}^q(\Omega)} \lim_{k\to\infty} \left\|\Pi_k^{\mathrm{div}} \boldsymbol{w} - \boldsymbol{w}\right\|_{\boldsymbol{L}^p(\Omega)} = 0.$$

Since $\left\|\Pi_k^{\mathrm{div}} \boldsymbol{w}\right\|_{\boldsymbol{L}^\infty(\Omega)} \le C \left\|\boldsymbol{w}\right\|_{\boldsymbol{L}^\infty(\Omega)}$, the strong convergence of $\mathbf{B}_n^{*(k)}$ gives

$$\lim_{k\to\infty} \left(\mathbf{J}_n^{(k)}, \mathbf{B}_n^{*(k)} \times \Pi_k^{\mathrm{div}} \boldsymbol{w}\right) = \lim_{k\to\infty} \left(\mathbf{J}_n^{(k)}, \boldsymbol{B}_n^* \times \Pi_k^{\mathrm{div}} \boldsymbol{w}\right) = \left(\boldsymbol{J}_n, \boldsymbol{B}_n^* \times \boldsymbol{w}\right).$$

Now collecting the limits for all terms in (B.14), we find that (4.5) holds for all $\boldsymbol{v} = \boldsymbol{w} \in \boldsymbol{C}_0^\infty(\Omega) \cap \boldsymbol{H}(\operatorname{div} 0, \Omega)$. For given $\boldsymbol{u}_n \in \boldsymbol{V}$ and $\boldsymbol{B}_n^* \in \boldsymbol{L}^q(\Omega)$, the left-hand side of (4.5) provides a bounded and linear functional acting on $\boldsymbol{v} \in \boldsymbol{V}$. By the denseness of $\boldsymbol{C}_0^\infty(\Omega)$ in $\boldsymbol{V}$, (4.5) also holds for $\boldsymbol{v} \in \boldsymbol{V}(\operatorname{div} 0)$. $\square$